The Astrophysical Journal, 684:395–410, 2008 September 1

ANALYTICAL THEORY FOR THE INITIAL MASS FUNCTION: CO CLUMPS AND PRESTELLAR CORES

Patrick Hennebelle
Laboratoire de Radioastronomie, UMR CNRS 8112, École Normale Supérieure et Observatoire de Paris,
24 rue Lhomond, 75231 Paris Cedex 05, France

and

Gilles Chabrier[1]
École Normale Supérieure de Lyon, CRAL, UMR CNRS 5574, Université de Lyon, 69364 Lyon Cedex 07, France
Received 2008 February 12; accepted 2008 May 4

ABSTRACT

We derive an analytical theory of the prestellar core initial mass function (IMF) based on an extension of the Press-Schechter statistical formalism. Our approach relies on the general concept of the gravothermal and gravoturbulent collapse of a molecular cloud, with a selection criterion based on the thermal or turbulent Jeans mass, which yields the derivation of the mass spectrum of self-gravitating objects in a quiescent or a turbulent environment. The same formalism also yields the mass spectrum of non-self-gravitating clumps produced in supersonic flows. The mass spectrum of the self-gravitating cores reproduces well the observed IMF. The theory predicts that the shape of the IMF results from two competing contributions, namely, a power law at large scales and an exponential cutoff (lognormal form) centered around the characteristic mass for gravitational collapse. The cutoff exists both in the case of thermal or turbulent collapse, provided that the underlying density field has a lognormal distribution. Whereas pure thermal collapse produces a power-law tail steeper than the Salpeter value, $dN/d\log M \propto M^{-x}$ with $x \simeq 1.35$, the latter is recovered exactly for the (three-dimensional) value of the spectral index of the velocity power spectrum, $n \simeq 3.8$, found in observations and in numerical simulations of isothermal supersonic turbulence. Indeed, the theory predicts that $x = (n+1)/(2n-4)$ for self-gravitating structures and $x = 2 - n'/3$ for non-self-gravitating structures, where n' is the power spectrum index of $\log\rho$. We show that, whereas supersonic turbulence promotes the formation of both massive stars and brown dwarfs, it has an overall negative impact on star formation, decreasing the star formation efficiency. This theory provides a novel theoretical foundation to understand the origin of the IMF and provides useful guidance to numerical simulations exploring star formation, while making testable predictions.

Subject headings: ISM: clouds — stars: formation — stars: luminosity function, mass function — turbulence

1. INTRODUCTION

Since the seminal work of Salpeter (1955) and its empirical derivation of the stellar initial mass function (IMF), defined as the number density of stars per log mass interval, $dN/d\log M$, tremendous effort has been devoted to the characterization of the IMF in various environments, including the Galactic field, young clusters, starforming regions, but also the Galactic bulge and halo or high-redshift galaxies, with the aim to identify the underlying physical mechanisms responsible for its behavior (see, e.g., Kroupa 2002; Chabrier 2003a, 2005 for recent reviews). A correct understanding of the IMF is one of the major, unresolved issues in astrophysics. Indeed, the IMF provides the essential link between stellar and galactic evolution and determines the chemical, light, and baryonic content of the universe. On the other hand, various observations of the prestellar dense core mass function (CMF) have shown its striking similarity with the stellar IMF, the former one being shifted by a factor of $\simeq$2–4 toward higher masses with respect to the latter one (Motte et al. 1998; Testi & Sargent 1998; Johnstone et al. 2000; André et al. 2007; Alfves et al. 2007). This strongly suggests that the IMF might already be determined by the CMF, at the prestellar stage, and thus would be due to the dynamics of the parent molecular gas. In the present paper we adopt this observationally supported perspective, and we refer without distinction to the CMF/IMF for the derivation of the general theory, except in § 7.1 where we specifically address this issue.

1.1. *Previous Works*

Various attempts, by many authors, have been made to derive a general theory for the IMF, with the aim to understand its origin and thus to make robust *predictions* for the stellar mass distribution under various conditions. These theories are based on analytical or numerical studies and, without being exhaustive, invoke either gravitational fragmentation or accretion (Silk 1995; Inutsuka 2001; Basu & Jones 2004; Bate & Bonnell 2005), turbulence (Padoan et al. 1997; Padoan & Nordlund 2002; Tilley & Pudritz 2004; Ballesteros-Paredes et al. 2006), purely independent stochastic processes (Larson 1973; Zinnecker 1984; Elmegreen 1997), or outflows (Adams & Fatuzzo 1996) as the dominant mechanism responsible for the CMF/IMF.

The CMF/IMF has been inferred from hydrodynamical simulations using either the smoothed particle hydrodynamics technique and sink particles (Bate & Bonnell 2005) or grid codes and clump-finding algorithms (Padoan & Nordlund 2002; Padoan et al. 2007; Tilley & Pudritz 2004; Li et al. 2004; Ballesteros-Paredes et al. 2006), but with different conclusions. Padoan et al. (2007) conclude that the CMF/IMF produced in purely hydrodynamical simulations is too stiff, compared with the Salpeter value, whereas Tilley & Pudritz (2004), performing a virial analysis, reproduce the Salpeter slope and Ballesteros-Paredes et al. (2006) find that the CMF/IMF depends on the Mach number. Padoan et al. (2007) also conclude that simulations including the presence

[1] Visiting scientist, Max Planck Institute for Astrophysics, Garching, Germany.

of a weak magnetic field yield the proper CMF/IMF and, thus, that the presence of a magnetic field is mandatory to recover the correct Salpeter high-mass tail.

Analytically, the most complete and successful approach to the derivation of the CMF/IMF has been proposed by Padoan & Nordlund (Padoan et al. 1997; Padoan & Nordlund 1999, 2002). It entails the following basic assumptions: protostellar cores result from overdensities due to shocks, and fluctuations of the underlying velocity field follow a Kolmogorov-like scale dependence. This enables them to obtain the mass of the cores as a function of the scale. Then, these authors invoke the fact that the number of cores should depend on the scale L as $\mathcal{N}(L) \propto L^{-3}$. Combining the latter relation with their mass scale dependence, they obtain a distribution of the number of objects per mass interval, $\mathcal{N} = dN/dM$, which follows a power law. As a last step, they combine this distribution with the distribution of Jeans masses obtained from the probability density function (PDF) of the field. One of their main conclusions is that in the hydrodynamical case, the slope of the CMF/IMF is too stiff compared with the Salpeter value, while the latter is recovered in the weakly magnetized case, due to different magnetized shock jump relations. This approach, although retaining undoubtedly some interesting concepts, presents various shortcomings. First of all, the $\mathcal{N}(L) \propto L^{-3}$ relation is not rigorously justified (see Elmegreen 2007). Furthermore, there is no proper integration over a fluctuation spectrum, and the Jeans mass distribution should not be independent of the core mass inferred from the shock conditions. The shock conditions themselves are not well justified for the magnetic case, since they assume that the magnetic field is always perpendicular to the shock. Finally, the result of the CMF/IMF being too stiff in the hydrodynamical case is in contradiction with the numerical simulations of Bate & Bonnell (2005) and Tilley & Pudritz (2004). At last, in the Padoan & Nordlund model, the turbulence is supposed to be taken into account implicitly in the shock velocity dependence and through the lognormal distribution of Jeans masses, but the turbulent support is *not* explicitly accounted for in this theory. In conclusion, none of the presently available analytical theories of the mass function provide a rigorous and robust foundation for the CMF/IMF.

1.2. *Aim of the Paper*

Such a robust theory has been derived in the cosmological context by Press & Schechter (1974, hereafter PS74), who have derived an analytical formulation of the number density of collapsing dark matter halos in the so-called hierarchical model of structure formation. In spite of its relative simplicity, this formalism has been shown to reproduce remarkably well the results of large computer simulations and has been applied successfully to various cosmological problems aimed at understanding galaxy formation. This formalism also provides precious guidance to observations or numerical simulations of structure formation in the universe. The first attempt to apply the PS74 formalism to the field of star formation was made by Inutsuka (2001). In the present paper we extend this formalism to the characterization of the CMF/IMF of stellar cores and of CO clumps, in the general picture of the gravothermal or gravoturbulent collapse of a molecular cloud, with a selection criterion based on the thermal or turbulent Jeans mass for the stellar CMF/IMF and on a simple density threshold for the CO clumps. Our analytical theory reproduces well the characteristic IMF derived from observations over the entire mass range from the high-mass to the brown dwarf domains, with the proper characteristic mass and Salpeter high-mass power-law exponent. We demonstrate that the CMF/IMF is obtained from the statistical selection involving hydrodynamical thermal or nonthermal motions, characterized by a lognormal density distribution, and gravitational instability, through the threshold condition for gravitational collapse, which sets up the characteristic mass. This interplay between hydrodynamics and gravity leads to the transition from the power-law tail at large masses to a lognormal form at small masses, as found in the IMF inferred from observations (Chabrier 2003a, 2005). In the presence of large-scale turbulent motions, the slope of the power-law tail is determined by the spectral index of the turbulent power spectrum, and the proper Salpeter exponent corresponds to the present-day observed value in molecular clouds. The characteristic mass and the variance of the lognormal part are entirely determined by the local conditions prevailing in the cloud, namely, the temperature, density, and thermal or turbulent rms velocity. Although based on the same general concept as the one suggested by Padoan & Nordlund (see references above), the present theory is more general and identifies shortcomings in these authors' approach. The paper is organized as follows: in § 2 we derive the framework of our statistical formalism; in § 3 we consider the simple density threshold and calculate the related mass spectrum of CO clumps; in § 4 we introduce the Jeans-type selection criterion. The general CMF/IMF analytical formulation is derived in § 5, while the results are presented in § 6. Section 7 is devoted to comparison with observations and with previous works. Section 8 concludes the paper. In order to facilitate the reading of the paper, the most important symbols and notations used in the paper are given in Table 1.

2. STATISTICAL DESCRIPTION

2.1. *PDF from Supersonic Turbulence*

In the PS74 theory of structure formation, the structures are identified with overdensities in a random field of density fluctuations,

$$\mathcal{P}(\delta) = \frac{1}{\sqrt{2\pi\sigma^2}} \exp\left(-\frac{\delta^2}{2\sigma^2}\right), \tag{1}$$

where $\delta = \rho/\bar{\rho} - 1$, $\bar{\rho}$ being the local mean density, and σ is the standard deviation of the distribution. However, whereas the density of the primordial universe is known to be very uniform, the density field in molecular clouds is highly nonuniform, which considerably increases the degree of complexity to derive an analytical formalism. On large scales ($\gtrsim$pc), the spectral line widths of molecular transitions observed in molecular clouds indicate highly supersonic motions characterized by Mach numbers $\mathcal{M} = \langle V^2 \rangle^{1/2}/C_s > 1$, where $C_s = (kT/\mu m_{\rm H})^{1/2} \approx 0.2(\mu/2.0)^{-1/2}(T/10\ {\rm K})^{1/2}$ km s^{-1} denotes the thermal sound speed and μ is the mean molecular weight.

The exact nature of the turbulence in molecular clouds is still a matter of debate. Numerically, it has been found that non-self-gravitating supersonic isothermal turbulence leads to density fluctuations which are Gaussian at all scales in terms of the *logarithm* of the density, $\delta = \log(\rho/\bar{\rho})$,[2] yielding a so-called lognormal distribution in density (Vázquez-Semadeni 1994; Padoan et al. 1997; Passot & Vázquez-Semadeni 1998; Ostriker et al. 2001; Kritsuk et al. 2007). More specifically, it has been inferred from numerical simulations that

$$\mathcal{P}(\delta) = \frac{1}{\sqrt{2\pi\sigma_0^2}} \exp\left[-\frac{\left(\delta - \bar{\delta}\right)^2}{2\sigma_0^2}\right], \tag{2}$$

where $\bar{\delta} = -\sigma_0^2/2$, from equation (2), and

$$\sigma_0^2 = \ln\left(1 + b\mathcal{M}^2\right) \tag{3}$$

[2] Here we adopt a different notation from the cosmological case, since δ is not the difference between the variable $\log(\rho/\bar{\rho})$ and its mean.

TABLE 1
VARIABLES

Variable	Description
x	Index of the IMF $dN/d\log M \propto M^{-x}$ (Salpeter index: $x = 1.35$)
n	Three-dimensional power spectrum index of the velocity field (Kolmogorov case: $n = 11/3$)
n'	Three-dimensional power spectrum index of the log density ($\log \rho$) field
η	Exponent of the velocity dispersion vs. size relation, $\eta = (n-3)/2$
L_i	Injection scale or system size
R	Smoothing scale
$\lambda_{\rm J}^0$	Jeans length
$\tilde{R}$	$R/\lambda_{\rm J}^0$
M	Cloud mass
$M_{\rm J}^0$	Jeans mass
$\tilde{M}$	$M/M_{\rm J}^0$
$\tilde{M}^*$	Mass at which thermal and turbulent support are comparable
$\bar{\rho}$	Cloud mean mass density
δ	Logarithmic contrast density $\log(\rho/\bar{\rho})$
$\mathcal{N}(M)$	$\mathcal{N}(M)dM = dN$ number density of stars of mass between M and $M + dM$
$\mathcal{N}_0$	$\bar{\rho}/M_{\rm J}^0$
$\mathcal{M}$	Mach number at the cloud scale
$\mathcal{M}_*$	Mach number at the Jeans scale
$\sigma(R)$	Width of the density distribution at scale R
σ_0	Width of the density distribution at scale L_i
C_s	Sound speed
$V_{\rm A}$	Alfvén speed
$V_{\rm rms}$	Root mean square velocity, $V_{\rm rms} = V_0(R/1\ {\rm pc})^\eta$
V_0	Root mean square velocity at $R = 1$ pc

with $b \approx 0.25$. In this expression, the Mach number $\mathcal{M}$ can be either a hydrodynamical or an Alfvénic Mach number.

Whether these equations accurately describe the dynamics of molecular clouds remains an open issue. In our approach, we nevertheless adopt these expressions for reference. In any event, our formalism and our results can easily be applied to other distributions.

2.2. *Scale Dependence of the Density PDF*

In the cosmological literature, the dependence of σ on the scale R at which the density field is smoothed has been established to be

$$\sigma^2(R) = \int_0^\infty \tilde{\delta}^2(k) W_k^2(R)\, d^3k, \qquad (4)$$

where W_k is some window function to be specified (see, e.g., Press & Schechter 1974; Bower 1991; Padmanabhan 1993) and $\tilde{\delta}(k)$ is the *density* power spectrum. This expression simply states how the variance of the density field is related to its power spectrum. In the context of molecular clouds, a similar approach, namely, the δ-variance, has been proposed by Stutzki et al. (1998) and Bensch et al. (2001).

Assuming that $\tilde{\delta}^2$ is proportional to $k^{-n'}$ and using a window function sharply truncated in the k-space, $W_k(R) = \theta(R^{-1} - k)$, where $\theta(z) = 1$ if $z > 0$ and 0 otherwise, one gets $\sigma^2(R) \propto R^{n'-3}$. This expression is consistent provided $n' < 3$, since otherwise the integral diverges at small k (Padmanabhan 1993).

Unfortunately, in the context of supersonic turbulence, the PDF stated by equation (2) does not entail any scale dependence, despite the fundamental need to specify the scale at which the quantity is measured. This is likely due to the fact that in turbulence the fluctuations are dominated by the large scales, and thus, as long as the measurement is done at a scale which is small compared to the injection length L_i, the deviation from equation (2) remains small. In the case of weakly compressible turbulence, the density field undergoes small fluctuations. Therefore, in that case, it is possible to refer to the cosmological results (Padmanabhan 1993) and to use the expression given by equation (4), as pointed out by Hennebelle & Audit (2007). When the turbulence is subsonic, the power spectrum index of the density field is known to be close to the Kolmogorov index obtained for the *velocity* power spectrum in incompressible turbulence, i.e., $n = 11/3$ (e.g., Bayly et al. 1992; Kim & Ryu 2005).[3] In that case, however, the integral will diverge at small k, as mentioned above, due to the fact that the larger scales contain most of the energy. Therefore, the integral must be truncated at the smallest values of k, $k_{\rm min} \sim 2\pi/L_i$, so that equation (4) becomes

$$\sigma^2(R) = \int_{2\pi/L_i}^\infty \tilde{\delta}^2(k) W_k^2(R)\, d^3k = \int_{2\pi/L_i}^{2\pi/R} \tilde{\delta}^2(k) 4\pi k^2\, dk = C\left[1 - \left(\frac{R}{L_i}\right)^{n'-3}\right], \qquad (5)$$

where C is some constant. Note that Hennebelle & Audit (2007) have numerically checked that this expression is reasonable.

In the case of supersonic turbulence, the power spectrum of $\log(\rho)$ has been calculated by Beresnyak et al. (2005) and Kritsuk (2007, private communication) in isothermal hydrodynamical and MHD simulations. The derived exponent, n', turns out to be close to the $n = 11/3$ value obtained in incompressible turbulence for the velocity field. Note that this is not the case for the exponent of the *density* field power spectrum which becomes much smaller when the Mach number increases (Beresnyak et al. 2005; Kim & Ryu 2005). Strictly speaking, in the case of supersonic turbulence, the use of equation (4) is questionable since it is valid only for a periodic function, which is unlikely to be the case for the density

[3] Note that, in the present paper, the indices n' and n of the power spectrum of the log density and velocity fields, respectively, refer to the three-dimensional value of the power spectrum. The usual one-dimensional Kolmogorov and Burgers (1974) values thus correspond to $n_{\rm 1D} = n - 2 = 5/3$ and $4 - 2 = 2$, respectively.

field within a spatially finite molecular cloud. However, more generally, $\sigma(R)$ must obey the following properties. First of all, $\sigma \rightarrow 0$ when $R \rightarrow L_i$; second of all, σ must tend toward the expression given by equation (5) when $\mathcal{M} \rightarrow 0$, implying $C = \sigma_0^2$; third, $\sigma \rightarrow \sigma_0$ when $R \ll L_i$.

Since $\sigma(R)$ is rather constrained and since the expression stated by equation (4) with $C = \sigma_0^2$ obviously satisfies all these constraints, it seems reasonable to assume that σ is still given by equation (5) even in the supersonic case. In any event, as is shown below, the exact dependence of σ on R is not a crucial issue for the derivation of the CMF/IMF, as long as the aforementioned conditions are satisfied. Note also that our results regarding the mass spectrum of structures defined by a density threshold will remain unchanged as long as $\sigma^2(R) = \sigma_0^2 f(1 - (R/L_i)^{n'-3})$, with f any positive and monotonically increasing function such that $f(0) = 0$.

Therefore, in the following, we consider the random field of density fluctuations as given by

$$\mathcal{P}_R(\delta) = \frac{1}{\sqrt{2\pi\sigma(R)^2}} \exp\left\{ -\frac{\left[\delta + \sigma(R)^2/2\right]^2}{2\sigma(R)^2} \right\}, \quad (6)$$

where σ is given by equation (5) with $C = \sigma_0^2$.

In our approach, the starforming clumps issued from these large-scale turbulent motions are thus identified with overdensities $\delta = \log(\rho/\bar{\rho})$. The mass associated with the overdensity at scale R is

$$M \simeq R^3 \rho = R^3 \bar{\rho} e^{\delta}, \quad (7)$$

so that $R = (M/\bar{\rho})^{1/3} \exp(-\delta/3)$. Note that since we use the sharp k-space filter, the relationship between R and M is ambiguous up to a factor of unity. It is important to note that, unlike in the PS74 formalism, the mass depends not only on the scale R but also on the variable δ, a consequence of the lognormal, instead of uniform, underlying density distribution.

3. MASS SPECTRUM OF STRUCTURES DEFINED BY A DENSITY THRESHOLD

Before we investigate the more complex case of self-gravitating objects, we first consider objects defined as in PS74 by a simple density threshold, ρ_c. In the PS74 formalism, the structures above this threshold will have collapsed at the time of interest and will have formed a gravitationally bound object. In our case, this is different since in the interstellar medium the gas is supported against gravitational collapse by various sources (see § 4). However, structures above some density threshold may either undergo thermal instability, as studied by Hennebelle & Audit (2007), or simply be revealed observationally because they have a sufficient abundance of CO molecules. In any case, it is interesting to investigate this case because of its simplicity and because there are now numerous observations of the CO mass spectrum.

The total mass, $M_{\rm tot}(R)$, of the gas which at scale R has a density larger than $\rho_c = \bar{\rho}\exp(\delta_c)$ is simply

$$M_{\rm tot}(R) = L_i^3 \int_{\delta_c}^{\delta_{\rm sup}} \bar{\rho} \exp(\delta) \mathcal{P}_R(\delta) d\delta, \quad (8)$$

where L_i is the size of the system assumed to be comparable to the injection scale. The value $\delta_{\rm sup}$ is not consequential on the results and will be assumed to be equal to infinity, $\delta_{\rm sup} \rightarrow \infty$, in the rest of the calculations. This total mass, $M_{\rm tot}(R)$, represents the mass of the structures of size larger than or equal to R and of mass larger than or equal to

$$M_R^c = \rho_c R^3. \quad (9)$$

We are interested in counting the structures having a mass equal to M_R^c. Some of these structures, however, have a nonzero probability to be included in larger structures which exceed the density criterion, and thus, the number of these structures cannot be straightforwardly obtained by requiring that the total mass they contain be equal to $M_{\rm tot}$. This is similar to the so-called cloud-in-cloud problem in the PS74 theory (Bond et al. 1991; Jedamzik 1995). We follow the approach of Jedamzik (1995) to handle this problem (see also Yano et al. 1996; Nagashima 2001).

Let $\mathcal{N}(M')dM'$ be the number density of isolated structures of mass between M' and $M' + dM'$, which satisfy the aforementioned density criterion. More precisely, these structures are the ones which at scale $R' \simeq (M'/\rho_c)^{1/3}$ would have a density $\bar{\rho} \simeq \rho_c$. The mass contained in such structures is $M'\mathcal{N}(M')dM'$. At scale $R < R'$, these structures contain regions whose density can be larger or smaller than ρ_c.

Let $P(M_R^c, M')$ be the mass fraction of a structure of mass M' which, at scale R, has a density above the critical density. The mass of the gas having a density larger than ρ_c at scale R and yet contained in a structure of mass M' as defined above is thus $M'\mathcal{N}(M')P(M_R^c, M')dM'$. This yields a second expression for $M_{\rm tot}(R)$,

$$M_{\rm tot}(R) = L_i^3 \int_{M_R^c}^{\infty} M'\mathcal{N}(M')P\left(M_R^c, M'\right)dM'. \quad (10)$$

As emphasized by Jedamzik (1995), the exact value of $P(M, M')$ depends on the choice of the window function and to some extent on the exact definition of a structure (see Yano et al. 1996). Jedamzik explored the influence of $P(M, M')$ and found that its value has some limited influence on the result. However, in the case of a window function sharply truncated in the k-space, Yano et al. (1996) argue that $P(M, M') = 1/2$. This stems from the fact that, in that case, the smaller region inside the larger region has an equal probability to be overdense or underdense than δ_c. Note that in the cosmological case, the Bond et al. (1991) result is exactly recovered if one assumes $P(M, M') = 1/2$. As demonstrated in Appendix C, it appears that the value inferred by Yano et al. (1996) is also applicable in our case, we take $P(M_R^c, M') = 1/2$.

Equating equations (8) and (10) and deriving the expression with respect to R, we obtain

$$\mathcal{N}(M_R^c) = -\frac{2\bar{\rho}}{M_R^c}\frac{dR}{dM_R^c}\left[\int_{\delta_c}^{\infty} \exp(\delta)\frac{d\mathcal{P}_R}{dR}d\delta\right]. \quad (11)$$

This yields the following expression for the mass distribution at scale R,

$$\mathcal{N}(M_R^c) = -\frac{2\bar{\rho}}{M_R^c}\frac{dR}{dM_R^c}\frac{1}{\sqrt{2\pi\sigma^2}}\frac{d\sigma}{dR}\int_{\delta_c}^{\infty} A(\delta, R)d\delta, \quad (12)$$

where

$$A(\delta, R) = \left(-1 + \frac{\delta^2}{\sigma^2} - \frac{\sigma^2}{4}\right)\exp\left(-\frac{\delta^2}{2\sigma^2} + \frac{\delta}{2} - \frac{\sigma^2}{8}\right), \quad (13)$$

and with the expression adopted in § 2.2,

$$\frac{d\sigma}{dR} = -\frac{n'-3}{2\sigma}\frac{\sigma_0^2}{R}\left(\frac{R}{L_i}\right)^{n'-3}. \quad (14)$$

The integral can be calculated analytically,

$$\int_{\delta_c}^{\infty} A(\delta, R)d\delta = \left(\delta_c + \frac{\sigma^2}{2}\right)\exp\left[-\frac{(\delta_c - \sigma^2/2)^2}{2\sigma^2}\right], \quad (15)$$

and is positive if $\delta_c > -\sigma^2/2 = \bar{\delta}$, as in PS74. As demonstrated in Appendix A, when $\delta_c < -\sigma^2/2$, which physically corresponds to a void instead of a cloud, $\delta_c + \sigma^2/2$ must be replaced by $-(\delta_c + \sigma^2/2)$ in equation (15), therefore ensuring the positivity of $\mathcal{N}(M)$.

With the aforementioned definition of M_R^c (eq. [9]), we get for the mass spectrum of structures defined by the density threshold δ_c:

$$\mathcal{N}(M_R^c) = \frac{\bar{\rho}}{(M_R^c)^2} \frac{(n'-3)\sigma_0^2}{3\sqrt{2\pi}\sigma^3} \left(\frac{M_R^c}{M_0}\right)^{(n'-3)/3} \left(\frac{\bar{\rho}}{\rho_c}\right)^{(n'-3)/3} \times \left(\delta_c + \frac{\sigma^2}{2}\right) \exp\left[-\frac{(\delta_c - \sigma^2/2)^2}{2\sigma^2}\right], \quad (16)$$

where $M_0 = \bar{\rho} L_i^3$ is the whole mass contained within a volume L_i^3 and $\rho_c = \bar{\rho} \exp(\delta_c)$. This expression is very similar to the one derived by PS74 in the context of a uniform density background. As in PS74, we identify a *power-law contribution* and a *Gaussian truncation* around the threshold δ_c, and we recover the fact that the fraction of bound objects of mass greater than M_R is proportional to $\delta_c - \bar{\delta}$. When the scale $R \to L_i$, then $\sigma \to 0$, and thus, there is also a Gaussian cutoff for large-mass structures. Note that in the limit when $\delta_c \to \bar{\delta} = -\sigma^2/2$, $\mathcal{N}(M) \to 0$ except if $\sigma \to 0$, which precisely occurs when $R \to L_i$. This implies that, when the threshold density $\delta_c \to \bar{\delta}$, all the mass lies within a unique structure of size L_i, as expected.

On the other hand, there is no cutoff for small mass structures, since they arise because of turbulent fluctuations which are scale-free. This remains valid as long as the turbulent cascade remains self-similar, which implies that the scale R must be large with respect to the dissipation scale. Another important difference with the PS74 formalism is that time dependence is not taken into account. This point is discussed in § 4.5 for the case of self-gravitating fluctuations. Here, we note that in the context of non-self-gravitating structures defined by a simple density threshold, no time evolution is required to compute the mass spectrum of these structures.

Equation (16) naturally yields the scaling relation $\mathcal{N}(M) \propto M^\beta$ with $\beta = -2 + (n'-3)/3$, so the power-law exponent is now affected by the spectral index characteristic of the logarithmic density power spectrum. This exponent is identical to the exponent obtained analytically by Hennebelle & Audit (2007, their eq. [15]) for subsonic turbulence and is in good agreement with the mass spectrum inferred from numerical simulations (Hennebelle & Audit 2007; Hennebelle et al. 2008; Heitsch et al. 2008). The exponent of the logarithmic density power spectrum has received only little attention, but as mentioned above, values around the Kolmogorov exponent, $n = 11/3$, have been inferred from numerical simulations (Beresnyak et al. 2005; Kritsuk 2007, private communication). For $n' = 11/3$, we get $\beta = -16/9 = -1.777$. This value is remarkably close to the slope of the mass spectrum inferred for the CO clumps (Blitz 1993; Heithausen et al. 1998; Kramer et al. 1998). This indicates that the CO clumps very likely have a turbulent origin. Note that in Hennebelle & Audit (2007), it was proposed that fluctuations of the warm neutral medium induced by a transonic turbulence are amplified by thermal instability once the density reaches the instability threshold. The present calculations indicate that the two mechanisms, namely, subsonic turbulence followed by thermal instability and supersonic turbulence, lead to similar mass spectra. It is therefore difficult from observations of the mass spectrum only to determine which process is dominant. Note that the two mechanisms are actually not exclusive from each other.

4. SELECTION CRITERION: THERMAL AND TURBULENT JEANS MASS

Unlike in the cosmological case, where the gas is very cold and not turbulent, the gas in the interstellar medium is supported by a combination of thermal pressure, turbulence, and magnetic field. In this section we examine these various supports, and we derive criteria to be fulfilled by the structures in order to collapse.

4.1. *Thermal Jeans Mass*

In order for a cloud to collapse, its mass must be larger than the thermal Jeans mass,

$$M_{\rm J} = a_{\rm J} \frac{C_s^3}{\sqrt{G^3\rho}} = a_{\rm J} \frac{C_s^3}{\sqrt{G^3\bar{\rho}}} \exp\left(-\frac{\delta}{2}\right) = M_{\rm J}^0 \exp\left(-\frac{\delta}{2}\right), \quad (17)$$

where

$$M_{\rm J}^0 = a_{\rm J} \frac{C_s^3}{\sqrt{G^3\bar{\rho}}} \approx 1.0 a_{\rm J} \left(\frac{T}{10\ {\rm K}}\right)^{3/2} \left(\frac{\mu}{2.33}\right)^{-1/2} \left(\frac{\bar{n}}{10^4\ {\rm cm^{-3}}}\right)^{-1/2} M_\odot, \quad (18)$$

where $a_{\rm J}$ is a dimensionless parameter of order unity which takes into account the geometrical factor. In the absence of turbulent support, the clumps with mass larger than a Jeans mass will eventually collapse and form gravitationally bound objects. This implies a lower limit on the local density fluctuation, $M \geq M_{\rm J} = M_{\rm J}^0 \exp(-\delta/2) \Rightarrow \delta \geq -2 \ln(M/M_{\rm J}^0)$.

Therefore, using equation (7), we obtain two equivalent conditions for the starforming collapsing structures,

$$M \geq M_R^c = a_{\rm J}^{2/3} \frac{C_s^2}{G} R, \quad \delta \geq \delta_R^c = -2 \ln\left(\frac{R}{\lambda_{\rm J}^0}\right), \quad (19)$$

where $\lambda_{\rm J}^0 = a_{\rm J}^{1/3} C_s/(G\bar{\rho})^{1/2} \approx 0.1 a_{\rm J}^{1/3} (T/10\ {\rm K})^{1/2} (\mu/2.33)^{-1/2} (\bar{n}/10^4\ {\rm cm^{-3}})^{-1/2}$ pc is the thermal Jeans length.[4]

An important difference with the case of § 3 is that the threshold now depends on the scale R. In particular, $\delta_R^c \to \infty$ as $R \to 0$. Physically, this means that it is more difficult to have a gravitationally unstable object at small scales because of the thermal support.

4.2. *Turbulent Jeans Mass*

If turbulence is significant, the turbulent support must be taken into account. As in Tilley & Pudritz (2004), we use the virial theorem to decide whether or not a structure is going to collapse. Neglecting the surface terms, the virial theorem can be written as

$$\frac{1}{2}\frac{d^2 I}{dt^2} \simeq 2E_{\rm cin} + E_{\rm pot} + (3P_{\rm th} + E_{\rm mag})\mathcal{V}, \quad (20)$$

where $\mathcal{V}$ is the volume and $E_{\rm cin}$ includes the contribution from turbulence, $\sim(1/2)\rho\langle V_{\rm rms}^2\rangle$, where $\langle V_{\rm rms}^2\rangle^{1/2}$ is the turbulent rms

[4] Strictly speaking, the thermal Jeans length is $\sqrt{\pi} C_s/(G\bar{\rho})^{1/2}$.

velocity. The quantity $E_{\rm pot}$ is the gravitational energy and $E_{\rm mag}$ is the magnetic energy. It is usually admitted that the structures which collapse are the ones having $d^2I/dt^2 < 0$, although this criterion is not entirely rigorous, in particular if we were to apply it to one specific object. It is, however, a reasonable approximation for a statistical approach over a large population of objects, as in the present context (see, e.g., McKee 1999; Dib et al. 2007a). This leads to

$$\langle V_{\rm rms}^2 \rangle + 3(C_s)^2 < -E_{\rm pot}/M. \tag{21}$$

Therefore, within our analytical formulation and our statistical description of the IMF, turbulent support can be included under the usual form of an effective sound speed (or equivalently effective pressure; Chandrasekhar 1951; Bonazzola et al. 1987; Vázquez-Semadeni & Gazol 1995),[5]

$$C_{s,\rm eff} = \left[(C_s)^2 + (1/3)\langle V_{\rm rms}^2 \rangle\right]^{1/2}. \tag{22}$$

The turbulent rms velocity is observed to follow a power-law correlation with the size of the region, the so-called Larson-type relations,

$$\langle V_{\rm rms}^2 \rangle = V_0^2 \left(\frac{R}{1\ {\rm pc}}\right)^{2\eta} \tag{23}$$

with $V_0 \simeq 1$ km s^{-1} and $\eta \simeq 0.4$–0.5 (Larson 1981). Note that, strictly speaking, the Larson relations are representative of the molecular gas at the whole cloud scale. Given the low efficiency of star formation and the relatively high densities at which star formation is observed to take place, $\bar{n} \sim 10^4$–10^5 g cm^{-3} (Motte et al. 1998; André et al. 2007), it is not clear whether the Larson relations are representative of star formation regions. Indeed, the observed line width versus size relation for prestellar massive cores in starforming regions shows slightly higher densities and velocity dispersions than predicted by the Larson relations (Caselli & Myers 1995). Therefore, the use of the Larson relations, although reasonable, should be considered as simply indicative.

Using the fact that $\langle V_{\rm rms}^2(R)\rangle = \int_{2\pi/R}^{\infty} P_V(\boldsymbol{k}) d\boldsymbol{k} \propto R^{n-3}$, where $P_V(k) \propto k^{-n}$ is the velocity power spectrum, and equation (23), the exponent η is related to the (three-dimensional) index of turbulence n by

$$\eta = \frac{n-3}{2}. \tag{24}$$

Note that, strictly speaking, the index of turbulence n which appears in this expression, which is related to the power spectrum of v, is not necessarily the same as the one previously introduced, n', which is related to the less standard power spectrum of $\log \rho$. However, as mentioned above, numerical simulations seem to find that both indices are rather similar.

The aforementioned values of η thus lie between the ones corresponding to a Kolmogorov, $\eta = 1/3$, and a Burgers (1974), $\eta = 1/2$, value, pointing to mildly to highly supersonic conditions in starforming clouds. Recent high-resolution simulations of nonmagnetized isothermal supersonic turbulence (Kritsuk et al. 2007) yield $\eta \sim 0.4$–0.45 ($n \sim 3.8$–3.9). In the limit where thermal support can be neglected (valid for massive stars), we obtain a turbulent Jeans mass

$$M_{\rm J,turb} = a_{\rm J} \frac{V_0^3}{\sqrt{3^3 G^3 \bar{\rho} \exp(\delta)}} \left(\frac{R}{1\ {\rm pc}}\right)^{3\eta}. \tag{25}$$

As for the pure thermal case, the structures which collapse in the turbulent case are the ones such that $M > M_{\rm J,turb}$, which now yields

$$M \geq M_R^c = a_{\rm J}^{2/3} \frac{V_0^2}{3G} \left(\frac{R}{1\ {\rm pc}}\right)^{2\eta} R,$$
$$\delta \geq \delta_R^c = \ln\left[\frac{a_{\rm J}^{2/3}}{3} \frac{V_0^2}{G\bar{\rho}R^2} \left(\frac{R}{1\ {\rm pc}}\right)^{2\eta}\right]. \tag{26}$$

4.3. *General Case*

In the general case where both thermal and turbulent supports contribute, the condition for collapse, $M > M_{\rm J}$, becomes

$$M > a_{\rm J} \frac{\left[(C_s)^2 + \left(V_0^2/3\right)(R/1\ {\rm pc})^{2\eta}\right]^{3/2}}{\sqrt{G^3 \bar{\rho} \exp(\delta)}}, \tag{27}$$

which, with equation (7), implies

$$M > M_R^c = a_{\rm J}^{2/3} \left[\frac{(C_s)^2}{G} R + \frac{V_0^2}{3G} \left(\frac{R}{1\ {\rm pc}}\right)^{2\eta} R\right], \tag{28}$$

$$\delta > \delta_R^c = \ln\left\{\frac{a_{\rm J}^{2/3}\left[(C_s)^2 + \left(V_0^2/3\right)(R/1\ {\rm pc})^{2\eta}\right]}{G\bar{\rho}R^2}\right\}. \tag{29}$$

An important point to be stressed is that, in our approach, we select the regions of the gas at the very early stages of star formation, which will collapse *in the future* because the combination of all supports is not sufficient to balance gravity. In particular, the dense cores themselves, which are observed not to be very turbulent, represent in our approach the (collapsing) evolution from a selected initially more dilute and turbulent piece of fluid. This piece of fluid, which fulfills our criteria for collapse, is properly accounted for in the present theory, while the observed prestellar cores represent a more evolved state, of which physical properties are not described in the present theory. Similarly, it is known that turbulence dissipates in about one crossing time, so one may worry about not taking this effect into account in the theory. This can be understood as follows: if a piece of fluid contains too much turbulence, it will expand and gravity will be unable to take over. On the other hand, if the turbulence is not sufficient, gravitational collapse will proceed eventually. The decay of turbulence does not affect this selection process, unless perhaps for the cases where turbulence is just sufficient to balance gravity.

4.4. *Magnetic Field*

The presence of a magnetic field, known to be dynamically significant in star formation (Crutcher 1999), will modify to some extent this general picture of the origin of the CMF/IMF. Taking into account the magnetic field in such a theory requires one to know exactly how magnetic field and density correlate. In numerical simulations, a broad correlation has been found between density and magnetic field, yielding $B \propto \sqrt{\rho}$ (Passot et al. 1995; Padoan & Nordlund 1999). Observationally, using Crutcher's (1999) data,

[5] Note that, because of the anisotropic nature of turbulent support, the effective sound speed formulation should represent an upper limit of the true nonthermal contribution.

Basu (2000; see also Myers & Goodman 1988) has shown that the magnetic intensity follows very closely the relation $B \propto \rho^{1/2}\Delta V$, where $\Delta V \equiv \langle V_{\rm rms}^2 \rangle^{1/2}$ is the velocity dispersion. This suggests that the Alfvénic Mach number, $\mathcal{M}_{\rm A} = \Delta V/V_{\rm A}$, where $V_{\rm A} = B/(4\pi\rho)^{1/2}$ is the Alfvén velocity, may be approximately constant in molecular clouds. Basu proposes an explanation based on magnetic flux and mass conservation and approximate mechanical equilibrium along the field lines. His calculation shows that the Alfvén velocity can be written as $V_{\rm A} = (V_{\rm A}^0/C_s)[(C_s)^2 + V_{\rm rms}^2/3]^{1/2}$. Application of the virial theorem (eq. [20]) yields

$$3C_s^2 + \langle V_{\rm rms}^2 \rangle + \frac{\langle V_{\rm A}^2 \rangle}{2} < -E_{\rm pot}/M. \tag{30}$$

Therefore, in order to take into account the magnetic support in equation (27), we just have to replace $[(C_s)^2 + V_{\rm rms}^2/3]$ by $[(C_s)^2 + V_{\rm rms}^2/3 + V_{\rm A}^2/6]$. Assuming the aforementioned dependence for the magnetic field, inclusion of magnetic support in our theory thus simply leads to an expression for the Jeans length and the Jeans mass which is proportional to the one derived in the hydrodynamical case. All the calculations conducted in this paper could thus, in principle, be generalized to the MHD case by, e.g., simply replacing a_J by $a_J[1 + (V_{\rm A}^0/C_s)^2/6]^{3/2}$ or, more generally, by simply rescaling the sound speed and the rms velocity by different factors.

The magnetic field also modifies the value of the Mach number which appears in the width of the lognormal distribution. This implies that, in this simple approach, the magnetic field, because of the magnetic support, reduces the width of the density PDF (Vázquez-Semadeni et al. 2005). Although a more realistic treatment in which the magnetic field distribution would be properly taken into account is strongly needed, it seems difficult to perform it at this stage. Meanwhile, the present approach has the virtue of simplicity, while based on observational arguments.

4.5. *Time Dependence Issue*

In the PS74 formalism, time dependence is accounted for by relating the collapse epoch of the perturbation to its density contrast. Although this somehow simplistic approach can be improved (see, e.g., Audit et al. 1997), it nevertheless yields satisfying results (Efstathiou et al. 1988; Lacey & Cole 1993).

In principle, such a time dependence could also be obtained in our case by selecting at a time t not the gravitationally unstable pieces of fluid, but rather the ones that had time to collapse and form a singularity. However, the time evolution is more complex in molecular clouds than in the cosmological case because of the various sources of support of the gas against gravitational collapse. Therefore, deriving the time at which collapse really occurs is a complicated task. Ignoring time dependence in our theory implies that the distribution of collapsing objects obtained at the very early stages by our threshold conditions is the one obtained once star formation is completed within the cloud of interest.

A related problem concerns the dense core formation, subsequent accretion, and possible merging (see Dib et al. 2007b; Peretto et al. 2007) not taken into account in a time-independent analysis. As emphasized in § 4.3, the present analysis relies on a simple *statistical counting* of the smallest pieces of fluid which are dominated by gravity. Dense cores will form out of these pieces by progressively accreting the related initial reservoir of mass. Our analysis excludes any external accretion of gas which is not included in this initial reservoir.

This lack of time dependence is certainly a limitation of the present theory. However, the agreement between this theory and the observed CMF/IMF, as shown below, seems to suggest that time evolution should not drastically affect the initial mass spectrum of collapsing structures.

5. MASS SPECTRUM OF SELF-GRAVITATING OBJECTS: DERIVATION OF THE CMF/IMF

5.1. *Analytic Formulation*

5.1.1. *Physical Assumptions*

Let us consider a region of scale R. The places where δ is larger than the above-derived critical threshold δ_R^c, as defined by equations (19), (26), and (29), contain more than one Jeans mass and are going to form stars of mass *smaller* than or equal to M_R^c.

This is because we assume that the final mass of the cores which form is equal to the mass associated with the clouds containing only one Jeans mass, since clouds which contain initially more than one Jeans mass are likely to fragment into several objects, whose number is more or less equal to the number of Jeans masses contained in the cloud. Therefore, all points which, at scale R, have a density contrast larger than δ_R^c are going to form structures of mass *smaller* than or equal to M_R^c. This can also be understood in the following way. Consider a cloud which at scale R contains about one Jeans mass, implying that its mean density at scale R is about M_J/R^3. At smaller scales, it may happen that the cloud is not uniform but is composed of smaller, denser cores embedded into a more diffuse envelope. If these denser cores contain one Jeans mass, the end product of the collapse is likely to be a cluster of objects whose mass is close to the mass of the smaller/denser cores and not to the mass of the object at scale R. We note here a fundamental difference with the cosmological case, where it is assumed that the mass of the final objects is equal to the mass of the biggest cloud which satisfies the appropriate conditions. This difference arises from the fact that the density contrast between the standard molecular gas and the star itself is about 18–20 orders of magnitude. Note that in our approach, as mentioned above, we neglect any further accretion on the prestellar cores. More precisely, it is assumed that most of the mass which will eventually be accreted onto the prestellar dense core is contained within the initial Jeans mass reservoir.

Given the above-derived threshold conditions for collapse, the places where δ is smaller than δ_R^c contain less than one Jeans mass. Eventually, these regions can either form a mass bigger than M_R^c or form no structure at all. Therefore, in the present context, what we are interested in is to find out the total mass, $M_{\rm tot}(R)$, which is going to form structures of mass M_R^c or less. As just mentioned, this corresponds to the places with a density fluctuation $\delta > \delta_R^c$.

5.1.2. *Analytical Expression*

The mass contained within structures of mass $M < M_R^c$ is equal to the mass of the gas which, smoothed at scale R, has a logarithmic density larger than δ_R^c. We have

$$M_{\rm tot}(R) = L_i^3 \int_{\delta_R^c}^{\infty} \bar{\rho} \exp(\delta) \mathcal{P}_R(\delta) d\delta. \tag{31}$$

In a way similar to the approach followed in § 3, the mass $M_{\rm tot}(R)$ can also be estimated by counting directly the self-gravitating clouds of mass *smaller* than M_R^c. The number of such structures is $\mathcal{N}(M')P(R, M')dM'$, where $\mathcal{N}(M')dM'$ is the density of structures of mass between M' and $M' + dM'$ and $P(R, M')$ is the probability to find a gravitationally unstable cloud of mass M'

embedded inside a cloud of gas which at scale R has a logarithmic density larger than δ_R^c. Therefore,

$$M_{\rm tot}(R) = L_i^3 \int_0^{M_R^c} M' \mathcal{N}(M') P(R, M') dM'. \quad (32)$$

Note that the integration is from 0 to M_R^c, because if a self-gravitating cloud of mass M contains a self-gravitating cloud of mass M', then, as explained previously, we assume that an object (or few objects) of mass M' will form instead of an object of mass M.

Estimating the probability $P(R, M')$ is not straightforward. It seems possible to formulate it in a way similar to Jedamzik's (1995) formulation of $P(M, M')$ in the cosmological case (his eqs. [8a] and [8b]). However, the complexity of the corresponding expression would lead to an equally complex result from which it would be difficult to extract the basic physical principles. On the other hand, Jedamzik finds significant deviation from the case $P(M, M') = 1/2$ only for structures 6–8 orders of magnitude smaller than M_*.[6] In the present case of interest, the IMF typically entails masses at most 3 orders of magnitude smaller than the mean Jeans mass. Therefore, it seems reasonable, in the present first step calculations, to follow the most simple approach. In the following, we thus assume that $P(R, M') = 1$. This means that we make the assumption that any self-gravitating cloud of mass smaller than M_R^c is embedded into a cloud which, smoothed at scale R, is Jeans unstable. In other words, we assume that the Jeans unstable clouds are not isolated but are embedded into bigger Jeans unstable clouds (containing more than one Jeans mass). This assumption is further justified in Appendix D. As is shown below by our results, this seems to be a very reasonable assumption.

Equating equations (31) and (32) and deriving the expression with respect to R, one gets

$$\mathcal{N}(M_R^c) = \frac{\bar\rho}{M_R^c} \frac{dR}{dM_R^c} \left[-\frac{d\delta_R^c}{dR} \exp\left(\delta_R^c\right) \mathcal{P}_R\left(\delta_R^c\right) + \int_{\delta_R^c}^{\infty} \exp(\delta) \frac{d\mathcal{P}_R}{dR} d\delta \right] \quad (33)$$

as the general expression for the number density distribution of starforming collapsing regions under the above-defined selection criterion for collapse.

As seen, two terms appear in equation (33). Since δ_R^c is a decreasing function of R, the first term is positive. The second term is identical to the one which appears in equation (11). As shown in Appendix B, this term becomes significant only when $R \simeq L_i$, i.e., when the size of the structures becomes comparable to the size of the system itself. Clearly, in this limit the precise dependence of σ on R becomes crucial and the statistical approach becomes rather questionable. From an even more fundamental point of view, this raises the question of the exact definition of the isolated fragmenting systems that are considered in this work and how they are connected to the surrounding medium. We thus ignore this second term in the following, except in § 6.3 where it cannot be avoided. This implies that the spatial scale R must be small compared to L_i or, equivalently, that the mass of the structures must be small compared to the mass of the system itself.

5.1.3. *The Normalization Problem*

In order to check whether the expression we get for the mass spectrum of collapsing structures is correctly normalized, we consider a situation where the injection scale $L_i \to \infty$. In this limit the system is infinite. Therefore, all its mass, $\bar\rho L_i^3$, will eventually collapse, because even a low-density piece of fluid is contained within a Jeans mass. Then, we must have

$$\bar\rho L_i^3 = L_i^3 \int_0^{\infty} \mathcal{N}(M) M \, dM, \quad (34)$$

which, with equation (31), leads to

$$\bar\rho L_i^3 = \bar\rho L_i^3 \int_{-\infty}^{\infty} \exp(\delta) \mathcal{P}_R(\delta) d\delta. \quad (35)$$

It is easily shown that the integral is equal to 1, since it represents all the mass within the system. Thus, the equality is satisfied and our expression is adequately normalized.

5.2. *Mass Spectrum with Purely Thermal Support*

In the case of pure thermal support, the mass spectrum of gravitationally bound objects derives from equations (12), (15), and (19), and equation (33) becomes, ignoring its second term,

$$\mathcal{N}(M_R^c) = \frac{2\bar\rho M_{\rm J}^0}{\left(M_R^c\right)^3} \frac{1}{\sqrt{2\pi}\sigma} \exp\left\{ -\frac{\left[2 \ln\left(M_R^c/M_{\rm J}^0\right)\right]^2}{2\sigma^2} - \frac{\sigma^2}{8} \right\}, \quad (36)$$

which can also be rewritten as

$$\mathcal{N}(\tilde M) = \frac{2\bar\rho}{M_{\rm J}^0} \tilde M^{-3-[2 \ln(\tilde M)]/\sigma^2} \frac{\exp(-\sigma^2/8)}{\sqrt{2\pi}\sigma}, \quad (37)$$

where $\tilde M = M/M_{\rm J}^0$ and $\mathcal{N}(\tilde M) d\tilde M = N(M) dM$.

We clearly see from equation (37) that the mass spectrum involves two contributions, namely, a power law with an index of -3 and a lognormal contribution given by the term $-2 \ln(\tilde M)/\sigma^2$. The first contribution is dominant when $M_\sigma^- \ll \tilde M \ll M_\sigma^+$, where

$$\tilde M_\sigma^{\pm} = \exp\left(\pm \frac{3}{2}\sigma^2\right), \quad (38)$$

whereas the latter one eventually becomes dominant both at very large ($M \gg M_\sigma^+$) and at very small ($M \ll M_\sigma^-$) masses, where it produces an exponential cutoff. The cutoff at small masses had been previously identified by Padoan et al. (1997). It arises from both the lognormal nature of the density distribution and the threshold condition for collapse (eqs. [19], [26], and [29]), as demonstrated in the present paper. This provides a rigorous foundation for this peculiar form of the power-law exponent of the CMF/IMF, sometimes invoked empirically in the literature (Miller & Scalo 1979).

This clearly demonstrates that the stellar CMF/IMF results from two contributions, a power law which dominates in the aforementioned mass range, and a lognormal form, which becomes important at very small and very large masses, as characterized by the transition mass $\tilde M_\sigma^{\pm}$ (eq. [38]). Equation (37) also shows that the mass spectrum of bound objects issued from a purely thermal collapse has a much steeper distribution at large masses, $\mathcal{N} \propto M^{-3}$, than the one given by the Salpeter CMF/IMF, $\mathcal{N}(M) \propto M^{-2.35}$. It also highlights the importance of the characteristic scale of the system on the mass spectrum, through the scale dependence of the variance σ (see § 2). Finally, it also clearly shows the

[6] Interestingly enough, the discrepancy seems to decrease when his n decreases and in particular when it becomes negative, which is the case for turbulent fluctuations.

importance of the Mach number on the mass spectrum of collapsing prestellar cores. Indeed, with equations (3) and (38), we get

$$\tilde{M}_{\sigma}^{\pm} = \left(1 + b\mathcal{M}^2\right)^{\pm 3/2}. \tag{39}$$

Small-scale motions, i.e., small values of σ, will hardly produce any object far away from the mean Jeans mass.

5.3. *Mass Spectrum with Purely Turbulent Support*

In the case when the clumps are supported dominantly by turbulent motions, equations (12), (15), (26), and (33) yield

$$\begin{aligned}\mathcal{N}(\tilde{M}) &= \frac{2\bar{\rho}}{M_{\rm J}^0}\frac{(1-\eta)}{(2\eta+1)}\mathcal{M}_*^{3/(2\eta+1)}\tilde{M}^{-3\alpha_1} \\ &\quad\times \exp\left\{-\frac{\left[\ln\left(\mathcal{M}_*^{\alpha_3}\tilde{M}^{2\alpha_2}\right)\right]^2}{2\sigma^2}\right\}\frac{\exp(-\sigma^2/8)}{\sqrt{2\pi}\sigma} \\ &= \frac{2\bar{\rho}}{M_{\rm J}^0}\frac{(1-\eta)}{(2\eta+1)}\mathcal{M}_*^{6/(\eta-1)}\tilde{M}'^{\,-3\alpha_1-[2(\alpha_2)^2/\sigma^2]\ln(\tilde{M}')} \\ &\quad\times \frac{\exp(-\sigma^2/8)}{\sqrt{2\pi}\sigma},\end{aligned} \tag{40}$$

where $\tilde{M} = M/M_{\rm J}^0$, $\tilde{M}' = \mathcal{M}_*^{3/(\eta-1)}\tilde{M}$, $\alpha_1 = (1+\eta)/(2\eta+1)$, $\alpha_2 = (\eta-1)/(2\eta+1)$, $\alpha_3 = 6/(2\eta+1)$, and

$$\begin{aligned}\mathcal{M}_* &= \frac{1}{\sqrt{3}}\frac{V_0}{C_s}\left(\frac{\lambda_{\rm J}^0}{1\ \rm pc}\right)^{\eta} \\ &\approx (0.8\text{–}1.0)\left(\frac{\lambda_{\rm J}^0}{0.1\ \rm pc}\right)^{\eta}\left(\frac{C_s}{0.2\ \rm km\ s^{-1}}\right)^{-1},\end{aligned} \tag{41}$$

where the ratio $(V_0/1\ \rm pc)^{\eta}$ is given by the aforementioned Larson relation (eq. [23]). Roughly speaking, the effective Mach number $\mathcal{M}_*$ measures the relative importance of turbulent versus thermal support contributions at the Jeans length scale. Note that, according to the discussion of § 4.4, this effective Mach number $\mathcal{M}_*$ can be renormalized to take into account the presence of a magnetic field. This requires, however, a proper knowledge of the exact dependence of both the uniform and fluctuating components of the magnetic field (or Alfvén velocity) on the thermal and nonthermal contributions of the velocity dispersion, respectively.

From comparison between equations (37) and (40), we first note that the introduction of the turbulent contribution into the effective sound speed modifies the exponent of the power-law term, through the Larson exponent. Interestingly enough, the aforementioned favored value for supersonic turbulence, $\eta \approx 0.4$ (Kritsuk et al. 2007), yields *exactly* the Salpeter coefficient, $dN/dM \propto M^{-(1+x)}$. Indeed, $1 + x = 3\alpha_1 = 2.33$, bracketed by the Burgers (1974), $3\alpha_1 = 2.25$, and Kolmogorov, $3\alpha_1 = 2.4$, values. Expressed as a function of the (three-dimensional) index of turbulence, n, with the help of equation (24), the power-law exponent of the mass spectrum as obtained in our calculations reads

$$x = \frac{n+1}{2n-4}. \tag{42}$$

As for the thermal case, the precise value of the turnover mass, around which the CMF/IMF evolves from the power-law to the lognormal form, depends on the value of σ and therefore on the Mach number $\mathcal{M}$. Larger Mach values will produce larger numbers of small-scale collapsing clumps.

The reason why the mass spectrum is stiffer when thermal support only is considered than when turbulent support is taken into account is simply because the turbulent support increases with the scale. Thus, a lot of intermediate to relatively large mass structures (of the order of or larger than the usual Jeans mass) which are unstable under purely thermal criteria are stabilized by turbulence. This support thus prevents fragmentation of these structures into several smaller structures, leading naturally to a shallower and broader mass spectrum in the high-mass ($M > M_{\rm J}^0$) domain.

5.4. *General Case*

In the general case, where both thermal and nonthermal supports contribute, the mass spectrum now reads, from equations (12), (15), (29), (28), and (33) where, as explained above, the second term has been dropped,

$$\begin{aligned}\mathcal{N}\left(\tilde{M}\right) &= 2\mathcal{N}_0\frac{1}{\tilde{R}^3}\frac{1}{1+(2\eta+1)\mathcal{M}_*^2\tilde{R}^{2\eta}}\frac{1+(1-\eta)\mathcal{M}_*^2\tilde{R}^{2\eta}}{\left(1+\mathcal{M}_*^2\tilde{R}^{2\eta}\right)^{3/2}} \\ &\quad\times \exp\left\{-\frac{\left[\ln\left(\tilde{M}/\tilde{R}^3\right)\right]^2}{2\sigma^2}\right\}\frac{\exp(-\sigma^2/8)}{\sqrt{2\pi}\sigma},\end{aligned} \tag{43}$$

where $\tilde{R} = R/\lambda_{\rm J}^0$, $\tilde{M} = M/M_{\rm J}^0 = \tilde{R}(1+\mathcal{M}_*^2\tilde{R}^{2\eta})$, $\delta_R^c = \ln[(1+\mathcal{M}_*^2\tilde{R}^{2\eta})/\tilde{R}^2]$, and $\mathcal{N}_0 = \bar{\rho}/M_{\rm J}^0$. This expression can also be rewritten as

$$\begin{aligned}\mathcal{N}(\tilde{M}) &= 2\mathcal{N}_0\frac{1}{\tilde{R}^6}\frac{1+(1-\eta)\mathcal{M}_*^2\tilde{R}^{2\eta}}{\left[1+(2\eta+1)\mathcal{M}_*^2\tilde{R}^{2\eta}\right]} \\ &\quad\times\left(\frac{\tilde{M}}{\tilde{R}^3}\right)^{-(3/2)-(1/2\sigma^2)\ln(\tilde{M}/\tilde{R}^3)}\frac{\exp(-\sigma^2/8)}{\sqrt{2\pi}\sigma},\end{aligned} \tag{44}$$

We see that the transition between the thermal- and the turbulent-dominated regimes occurs when the radius $\tilde{R} \simeq \mathcal{M}_*^{-1/\eta}$ and, thus, for masses around

$$\tilde{M}^* \simeq 2(\mathcal{M}_*)^{-1/\eta}. \tag{45}$$

For $\mathcal{M}_*^2 \simeq 2$, we get $\tilde{M}^* \simeq 0.8$–1. At masses larger than $\tilde{M}^*$, we recover the power-law behavior characteristic of the turbulent collapse, with the proper Salpeter value. This is easily verified for the case $\eta = 0.5$, which yields $\mathcal{N}(\tilde{M})_{\tilde{M}\gg 1} \propto \tilde{M}^{-9/4}$. The small-mass limit (i.e., $\tilde{M} \ll \tilde{M}^*$), on the other hand, resembles the one of the purely thermal case. Therefore, at least for values of $\mathcal{M}_*$ of the order of unity, we expect the mass spectrum of collapsing structures in the general case to be bracketed by the turbulent and thermal behaviors at large and small scales, respectively.

6. RESULTS

In this section we study equation (44) and its dependence on the parameters, $\mathcal{M}$ (which enters the expression of σ) and $\mathcal{M}_*$. Recalling that the Mach number $\mathcal{M}$ is the ratio of velocity dispersion over sound speed at the scale of the *whole cloud*, whereas $\mathcal{M}_*$ is the ratio of velocity dispersion over sound speed at the scale of the *Jeans length*, we see that both parameters depend on the velocity dispersion. The first one increases with the size of the cloud, while the second one increases with the size of the Jeans length. In order to investigate their respective influence on the CMF/IMF, we first vary one of these two parameters while keeping the other one constant. Physically speaking, this corresponds to either considering clouds of fixed density but of various sizes ($\mathcal{M}$ varies but not $\mathcal{M}_*$), or changing the density but not the size ($\mathcal{M}_*$ varies but not $\mathcal{M}$). For the sake of simplicity, we assume in these two cases that $\sigma = \sigma_0$.

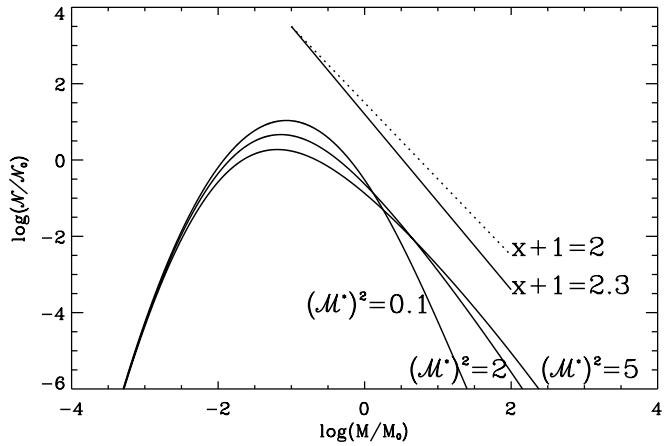

FIG. 1.—Mass spectrum for $\mathcal{M} = 6$ and various values of $\mathcal{M}_*^2$. For reference, power-law distributions $dN/dM \propto M^{-(x+1)}$ are also plotted for $x + 1 = 2$ and 2.3, about the Salpeter value.

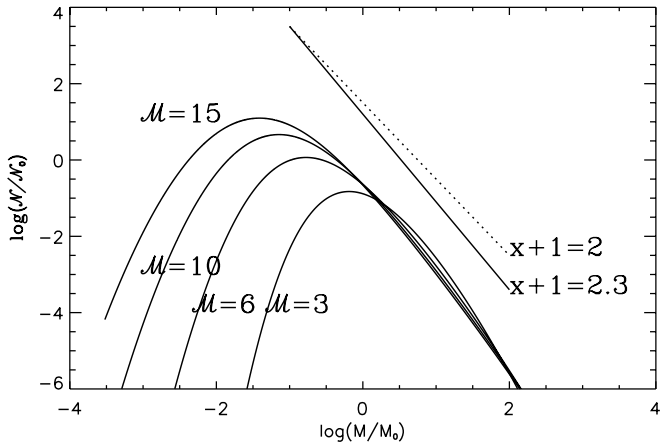

FIG. 2.—Mass spectrum for $\mathcal{M}_*^2 = 2$ and various values of $\mathcal{M}$.

Finally, in order to investigate the influence of turbulence on star formation, we simultaneously vary $\mathcal{M}$ and $\mathcal{M}_*$ while keeping their ratio constant. This latter case corresponds to a cloud of fixed size and density but of varying velocity dispersion. In this case, the dependence of $\sigma(R)$ on R is properly taken into account.

The results are expressed in terms of $M_{\rm J}^0$ as defined by equation (18). Typically, for a cloud of density $\bar{n} \simeq 10^3$ cm^{-3}, $M_{\rm J}^0$ is about 3 $M_\odot$. For clouds of size $\simeq$1–2 pc following the Larson laws, typical Mach number values are $\mathcal{M} \sim 6$. Typical values of $\mathcal{M}_*^2$ are around 1–2. These numbers must be considered as indicative, given the large uncertainties that remain on the exact conditions for star formation. In the following, the value of η is taken to be equal to 0.4.

6.1. *Thermal and Turbulent Support*

Figure 1 portrays the mass spectrum obtained in the general case (eq. [44]), for different values of $\mathcal{M}_*$, namely, $\mathcal{M}_*^2 = 0.1, 2,$ and 5, at a fixed Mach number $\mathcal{M} = 6$. For the first value of $\mathcal{M}_*$, the influence of the turbulent support is negligible ($\tilde{M}_* \simeq 30$) and the collapse is almost purely thermal. We see the steep cutoff at large masses due to the $\alpha = -3$ exponent in the power law, as well as the sharp exponential cutoff at small masses. As mentioned above, this latter term derives from the general formalism and from the critical density selection criterion and, thus, is *not* specifically due to turbulence, but to the lognormal distribution characteristic of the density field.

As expected, for $\mathcal{M}_*^2 = 2$ the behavior at small masses is almost identical to the purely thermal case. The CMF/IMF peaks at almost the same position, although fewer intermediate-mass stars form because of the turbulent support, which prevents the collapse of large structures into smaller ones. At large masses, the CMF/IMF is less stiff than for the pure thermal case and has an index close to the Salpeter value, as mentioned above. In the case $\mathcal{M}_*^2 = 5$, the number of intermediate-mass stars is even smaller, but the peak of the CMF/IMF remains weakly affected (as expected from eq. [45]).

6.2. *Influence of the Mach Number* $\mathcal{M}$

Figure 2 shows the CMF/IMF for $\mathcal{M}_*^2 = 2$ and various values of the Mach number $\mathcal{M}$. We stress that, since $\mathcal{M}_*$ is maintained as a constant, increasing the Mach number is not equivalent to increasing the value of V_0, but rather the size of the cloud.

Clearly, supersonic turbulence strongly enhances the collapse of small-scale structures while the number of large-scale structures does not change significantly (for these values of $\mathcal{M}$). This stems from the fact that the transition mass, M_σ^-, defined by equation (38), is modified by the variance σ, so that the exponential cutoff occurs at much smaller masses, for a given hydrodynamic Mach number $\mathcal{M}$, than for the thermal case.

This shows that, if large-scale motions in molecular clouds are strongly supersonic, they will produce a large population of brown dwarfs. It is the fact that small-scale structures become subsonic (eq. [23]), and thus of a dominantly thermal nature, that they hardly form gravitationally bound objects far away from the mean Jeans mass, and thus that brown dwarfs, although issued from the same general formation mechanism, are not formed as efficiently as (low-mass) stars around the mean Jeans mass. In the high-mass regime, as mentioned above, turbulence yields a shallower power-law tail than for thermal collapse. Mach number values $\mathcal{M} \sim 6$ yield the correct Salpeter index already for $M \gtrsim M_{\rm J}^0$, for a power spectrum index $n \simeq 3.8$ ($\eta \simeq 0.4$), as inferred from recent high-resolution simulations of supersonic turbulence (Kritsuk et al. 2007). As expected, the general case indeed lies between the turbulence-dominated collapse behavior at large masses and the thermal behavior at small scales. Not surprisingly, the characteristic mass of the spectrum is fixed by the characteristic mass for collapse, affected to some extent by the Mach number (which enters the variance), illustrating the role played by gravity in this collapse gravohydrodynamical picture.

6.3. *Support versus Turbulent Triggering*

A key, yet unsettled issue in the modern picture of star formation is to clearly understand the overall effect of turbulence on this process. On the one hand, turbulence creates density enhancements (obviously related to $\mathcal{M}$, as given by eq. [39]) which tend to favor gravitational instability. On the other hand, the turbulent support tends to stabilize the gas (the turbulent support is due to $\mathcal{M}_*$ in our theory). Figures 1 and 2 show how the CMF/IMF changes with $\mathcal{M}$ and $\mathcal{M}_*$. However, if one increases the level of turbulence in a cloud of fixed size and mass, both parameters should change, while their ratio should remain constant. Figure 3 displays the mass spectrum obtained for three values of $\mathcal{M}$, namely, $\mathcal{M} = 3$, 6, and 12, while keeping $\mathcal{M}/\mathcal{M}_* = \sqrt{3}(L_i/\lambda_{\rm J}^0)^\eta$ constant and equal to $6/\sqrt{2}$ (i.e., $\lambda_{\rm J}^0/L_i \simeq 0.1$), leading to $\mathcal{M}_*^2 =$ 0.5, 2, and 8, respectively. As expected, we obtain a combination of the behaviors observed in Figures 1 and 2: the smaller the values of $\mathcal{M}$ and $\mathcal{M}_*$, the narrower the mass range of star formation around the characteristic mass $M_{\rm J}^0$. Conversely, large Mach numbers promote the formation of a larger number of low-mass and high-mass stars, but produce fewer stars around $M_{\rm J}^0$.

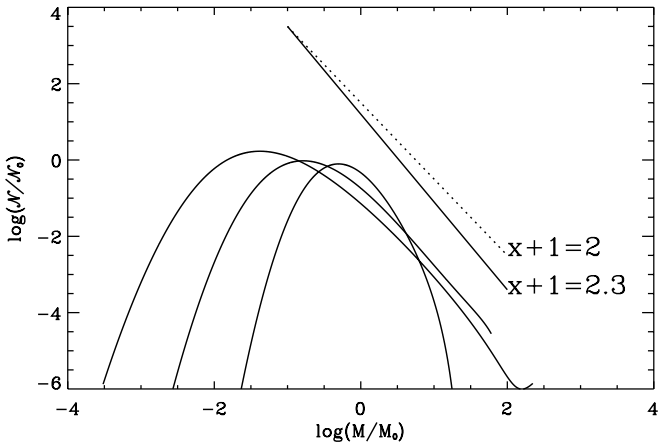

FIG. 3.—Mass spectrum for various values of $\mathcal{M}$ and $\mathcal{M}_*$ for a constant ratio $\mathcal{M}/\mathcal{M}_* = 4.24$. Values of $\mathcal{M}$ correspond to 3, 6, and 12 from the narrower to the broader distributions, respectively.

Another important issue is to determine whether turbulence is globally promoting or quenching star formation (Krumholz & McKee 2005). Numerically (e.g., Mac Low & Klessen 2004), it has been found that the global effect of turbulence on star formation is negative, although the turbulent support is much more effective if the driving is imposed at small scales. To verify this conclusion, we have computed the total mass density included in the gravitationally bound prestellar cores, $M_{\rm tot}/\mathcal{V} = \int \mathcal{N}(M) M\, dM$, for various values of $\mathcal{M}$ and various values of $\mathcal{M}/\mathcal{M}_*$, namely, 6, $6/\sqrt{2}$, $6/\sqrt{3}$, $6/\sqrt{4}$, and $6/\sqrt{5}$, which correspond to $\lambda_{\rm J}^0/L_i \simeq 0.04$, 0.1, 0.18, 0.25, and 0.33, respectively. For these calculations, we have included the previously neglected second term in equation (33) and, thus, use the complete relation for $\mathcal{N}(M)$. As explained in § 5.1.3, the integral $\int_0^\infty M\mathcal{N}(M)dM$ is constant. In reality, however, the system has a finite mass and size, so that the integral must be truncated when $R \simeq L_i$ or, equivalently, when $M \simeq \bar{\rho} L_i^3$. Thus, the value of the integral depends on the injection scale. As discussed above, integrating until $R = L_i$ is questionable, and we thus stop the integration at $R = 2L_i/3 = L_{\rm cut}$. We have verified that using different values of $L_{\rm cut}$ yields the same trends and qualitatively similar results. Quantitatively speaking, however, the results obviously depend on the value of R at which the integration is stopped.

Figure 4 portrays the results of this global star formation efficiency as a function of the Mach number $\mathcal{M}$. The top curve corresponds to the largest value of $\mathcal{M}/\mathcal{M}_*$, i.e., the smallest value of $\lambda_{\rm J}^0/L_i$, whereas the bottom curve corresponds to the opposite. We see that, for a fixed value of $\mathcal{M}/\mathcal{M}_*$, the higher the Mach number, the smaller the star formation efficiency. In the same vein, for a given Mach number, the higher $\mathcal{M}_*$, the less efficient the star formation. These behaviors are in agreement with and provide a theoretical foundation to what has been inferred from numerical simulations. We stress that, quantitatively, these results depend on the choice of $L_{\rm cut}$. They demonstrate, however, that turbulence largely decreases the efficiency of star formation.

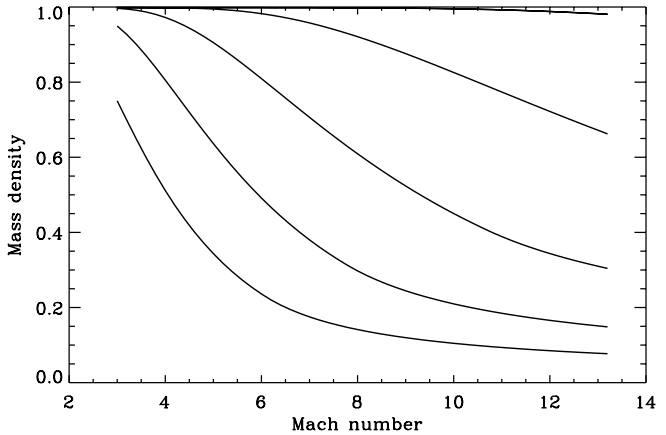

FIG. 4.—Total mass density over the initial mass density as a function of the Mach number $\mathcal{M}$ for various values of $\mathcal{M}/\mathcal{M}_*$ (see text; decreasing from top to bottom).

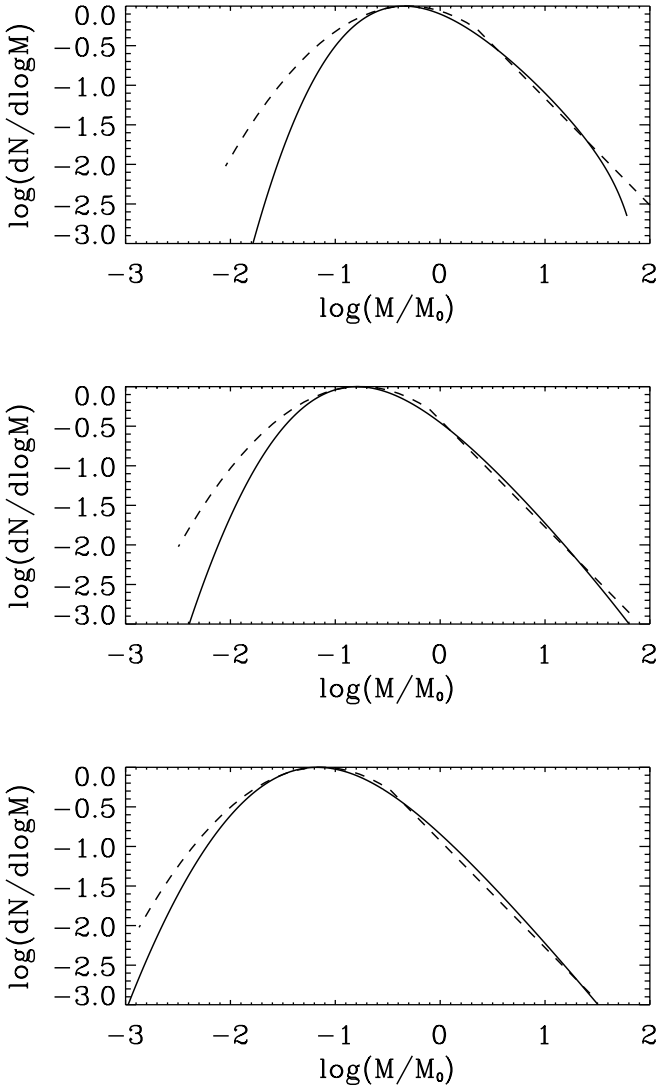

FIG. 5.—Comparison between the theoretical IMF/CMF, $dN/d\log M$ (*solid line*), obtained with $\mathcal{M} = 6$ (*top*), 12 (*middle*), 25 (*bottom*), and $\mathcal{M}_*^2 = 2$ and the stellar/brown dwarf *system* IMF (*dotted line*) of Chabrier (2003a). The peak of this latter IMF has been adjusted arbitrarily to the one of each theoretical mass function.

7. DISCUSSION

7.1. *Comparison with Observations*

7.1.1. *The Shape of the CMF/IMF*

Figure 5 compares our analytical CMF/IMF (eq. [44]) for three values of the Mach number, namely, $\mathcal{M} = 6$, 12, and 25, with the IMF representative of the Galactic field and young clusters (Chabrier 2003a). The latter reflects the so-called *system* IMF, since in general, present limitations on angular resolution do not allow one to resolve these systems into individual objects. On the other hand, our calculations are representative of the early stages

of the collapse and do not consider possible subsequent subfragmentation of the prestellar cores into multiple objects. The same is true for most of the present numerical simulations of star formation. In order to facilitate the comparison between the theoretical and the observationally derived distributions, the latter has been shifted in order to match the position of the peak of the analytical distribution. We come back to this point below. The general agreement between the two types of distributions is striking. In particular, the transition between the power-law tail and the lognormal form is very well reproduced. This clearly assesses the validity of such a composite functional form for the stellar IMF, whose physical foundation has been demonstrated in the present paper. At the low-mass end, the theoretical and observationally derived mass spectra start to differ noticeably below some mass value which depends on the Mach number, as analyzed in § 6. A value of $\mathcal{M} = 6$ leads to a deficit of both very massive stars and brown dwarfs compared with the observed distribution, because of the too restricted mass range between the high-mass and the low-mass exponential cutoffs. A value of $\mathcal{M} = 12$ improves the situation and yields a fairly reasonable agreement with the observational distribution, although still underestimating the number of very small ($\lesssim 10^{-2}\ M_\odot$) brown dwarfs. A value of $\mathcal{M} = 25$ yields a good agreement with the observationally derived mass spectrum over basically all the observationally probed mass domain. Although values of $\mathcal{M} \simeq 25$ are substantially larger than the ones usually associated with typical starforming regions, $\mathcal{M} \sim 6$–12, two important points need to be considered in these comparisons.

First of all, the statistics of brown dwarf detections below $\sim 10^{-2}\ M_\odot$ are still small, and determinations of the brown dwarf densities remain hampered by both observational (magnitude-limited samples, spectral-type effective temperature conversions, etc.) and theoretical (mass-age-L-$T_{\rm eff}$ determinations) uncertainties. The observationally derived IMF in this domain thus retains a large degree of uncertainty.

Second of all, the relation between the variance of the PDF obtained by turbulence, which determines the width of the CMF/IMF, and the Mach number is given by equation (3), with $b = 0.25$. This relationship is extracted from three-dimensional simulations of *isothermal* turbulence (Padoan & Nordlund 2002). Simulations taking into account a detailed treatment of the thermal properties of the gas in the molecular cloud, however, lead to an equation of state softer than isothermal, $P \propto \rho^{0.7}$–$\rho^{0.8}$, at least up to densities of a few 10^3 cm^{-3} (Glover & Mac Low 2007). We thus expect a larger dispersion of the PDF and, thus, a larger extension of the CMF toward small masses with a more compressible nonisothermal gas, for the same Mach number. Furthermore, recent numerical simulations of supersonic turbulence with compressible driven modes predict a significantly broader PDF, for the same rms Mach number, than simulations with rotationally driven modes, like the ones of Padoan & Nordlund (W. Schmidt 2007, private communication). These results suggest that equation (3) somehow underestimates the aforementioned value of b and, thus, the variance σ for a given $\mathcal{M}$. Finally, self-gravity could also possibly broaden the density PDF, as supported by numerical simulations (see, e.g., Vázquez-Semadeni et al. 2008), although the densest part of the density distribution in that case departs from a pure lognormal form. Consideration of these issues should improve the quantitative agreement between the present theory and observations.

7.1.2. *From the CMF to the IMF: The Core-to-Star Formation Efficiency*

As mentioned above, the theoretical and observationally derived mass functions, $dN/d\log M$, have been arbitrarily adjusted peak-to-peak. After the shape of the CMF/IMF, we now examine the agreement between the real positions of the peaks of the CMFs, which define the most probable stellar mass scale. The comparison with the observationally derived IMF on a solar-mass scale, however, depends on the exact value of the Jeans mass which, in our approach, defines the characteristic mass for collapse. Given the fact that the observationally derived system IMF peaks at roughly 0.3 $M_\odot$, this would imply that the Jeans mass should be about 1 $M_\odot$ for $\mathcal{M} = 6$ and $\sim$3 $M_\odot$ for $\mathcal{M} = 25$.

On the other hand, observations of prestellar condensations, as identified in dust continuum surveys, show that the CMF peaks at a mass about 3 times larger than the observational IMF, even though this peak determination still suffers from large uncertainties (Motte et al. 1998; Alves et al. 2007, André et al. 2007, 2008). Given the similarity of the shapes of the CMF and the IMF, this implies that the transformation of gravitationally bound prestellar condensations into genuine stellar or brown dwarf systems involves some *uniform* star formation efficiency factor, $\epsilon = M_\star/M_{\rm core}$, observed to be in the range $\epsilon \sim 30\%$–50%. Clearly, the process(es) responsible for the evolution of the CMF into the IMF remains ill determined, although magnetically driven outflows, expected to produce a mass-independent star formation efficiency factor in the appropriate range (Matzner & McKee 2000), offer an appealing explanation. This implies that the above estimate for the Jeans mass value adequate to match the observed IMF must be further increased by a factor of the order of $\sim$3, yielding $M_{\rm J}^0 \simeq 3\ M_\odot$ for $\mathcal{M} = 6$ and $M_{\rm J}^0 \simeq 10\ M_\odot$ for $\mathcal{M} = 25$.

7.1.3. *Physical Conditions*

Equation (18) shows that, for starforming core conditions $\mu = 2.33$, $T = 10$ K, and $\bar{n} = 10^3$ cm^{-3}, the Jeans mass is about 3 $M_\odot$, whereas it is about 1 $M_\odot$ for $\bar{n} = 10^4$ cm^{-3}. Fluctuations around these temperature and density values, as well as geometrical factors, however, will affect this determination to some degree, moving around the peak of the theoretical mass spectrum on a solar-mass scale. This would be consistent with the IMF being determined at gas densities in this density range. However, as discussed in § 4.4, the presence of a magnetic field increases the critical mass for collapse, moving the peak of our CMF, normalized to the standard thermal Jeans mass (eq. [18]), to larger masses. Estimates of the critical magnetized mass for collapse, as done in various seminal works and textbooks (e.g., Spitzer 1978; Lequeux 2005), predict values for the relevant magnetic Jeans mass, $M_\Phi \propto B^3/n^2$, of the order of $\sim$10 $M_\odot$ for $\bar{n} = 10^3$ cm^{-3} and $B = 10\ \mu$G. This implies that the typical gas density to produce a magnetic Jeans mass compatible with a peak of the CMF around 1 $M_\odot$, as found observationally, should be higher than 10^3 cm^{-3}, with a typical value of the magnetic field slightly larger than 10 μG. This is consistent with the densities characteristic of starforming clumps, $\bar{n} \sim 10^4$–10^5 cm^{-3} (André et al. 2007; Motte et al. 2007). On the other hand, the nice correlation observed by Basu (2000) suggests that the magnetic field also depends on the velocity dispersion. According to the analysis of § 4.4, this implies that only the *uniform* magnetic component should enter our Jeans mass determination. Unfortunately, the value of this component is not determined observationally. Clearly, more knowledge on the structure of the magnetic field and its correlation with density and velocity is required at this stage in order to determine more precisely the value of the magnetic Jeans mass and to make a precise comparison between the characteristic mass scales, and thus the peak positions, of the theoretically and observationally derived IMFs.

7.1.4. *Expected Dependence of the Peak Position in the Cloud Mass*

One surprising piece of observational evidence is that the peak of the IMF is fairly constant from one region to another (e.g.,

Chabrier 2003a, 2005; Luhman 2004, 2007; Moraux et al. 2005). Here, we investigate how the peak of the IMF depends on the mass of the cloud. Since, as emphasized above, the peak occurs in the thermally dominated regime, we simply take the derivative of $\mathcal{N}$ as given by equation (37), with respect to M, which yields

$$\tilde{M}_{\rm peak} = \exp\left(-\frac{3}{4}\sigma^2\right) = \frac{1}{\left(1+b\mathcal{M}^2\right)^{3/4}}. \quad (46)$$

This indicates that, for clouds characterized by high Mach numbers, the peak of the CMF is roughly proportional to $\mathcal{M}^{-3/2}$. Combined with equation (23), this gives $\tilde{M}_{\rm peak} \propto L^{-3/2\eta}$. Since, typically, the CO clump density varies with their size as $\rho \propto L^{-a}$, with $a = 0.7$–1 (Larson 1981; Heithausen et al. 1998), we get

$$M_{\rm peak} = M_{\rm J}^0 \tilde{M}_{\rm peak} \propto L^{(-3/2)\eta + a/2}. \quad (47)$$

For $\eta = 0.5$ and $a = 1$ or for $\eta = 0.4$ and $a = 0.7$, we find the same value $(-3/2)\eta + a/2 = -0.25$, while for $\eta = 0.5$ and $a = 0.7$, $(-3/2)\eta + a/2 = -0.4$. Since typically $M \propto L^{2-2.3}$ in these objects, we find that $M_{\rm peak} \propto M^{0.1}$–$M^{0.2}$. Thus, changing the mass of the clump by a factor 10^2 changes the location of the peak of the IMF by a factor less than $\simeq 2$. This partial compensation between the comparable increasing and decreasing scale dependences of the Mach number and the Jeans mass, respectively, may be one of the reasons why the peak of the IMF appears to be rather constant over a wide range of stellar cluster conditions (see also Elmegreen et al. 2008).

7.2. *Comparison with Previous Works*

Although based on the same underlying picture of hydrodynamically or turbulence-driven fragmentation, the theory presented in this work is more general than the one proposed by Padoan & Nordlund (2002). First of all, the present theory does not invoke shock conditions whose validity might be questionable, since they assume that the magnetic field is perpendicular to the shock. Note that, under this assumption, the shock jump conditions imply that $B \propto \rho$, which is not compatible with the observations. Second of all, the present theory does not assume a one-to-one correspondence between the probability distribution of the turbulent gas density and that of local Jeans masses, identified as collapsing protostars. Regions of the gas which will collapse into a gravitationally bound object are properly accounted for, as they must fulfill the Jeans mass criterion through the proper selection condition for the density threshold. Regions where density fluctuations fail to fulfill this criterion will not be included into the mass spectrum distribution of collapsing objects. Therefore, the theory ensures a correct counting of the collapsing structures. Finally, turbulent or magnetoturbulent support enters explicitly in our theory, whereas it is interesting to note that this is not the case in the Padoan & Nordlund theory. Note that their original CMF/IMF (Padoan et al. 1997) closely resembles our pure thermal case. It is very likely the reason why, in the pure hydro case, their high-mass tail is dominated by the steep $dN/dM \propto M^{-3}$ power law, yielding an underestimate of the number of massive stars relative to low-mass ones.

As in the Padoan & Nordlund theory, we recover the fact that the CMF/IMF is shaped by the product of two contributions, namely, a power-law form, which dominates at intermediate scales, and two exponential cutoffs, one below about the characteristic mass for collapse and one at large scales. However, we note that this low-mass cutoff is not the result of turbulence, but is the result of the Gaussian, more precisely the lognormal distribution of the density field, and of the threshold condition for collapsing structures. Although turbulence does produce such a distribution type, other mechanisms, like wave propagation or gravity, could presumably lead to similar distributions. Turbulence, however, leads to a significantly smaller value for the low-mass cutoff, compared with the thermal case, promoting the formation of low-mass objects, in particular brown dwarfs. We also note that in the Padoan & Nordlund theory, the high-mass part of the IMF is a pure power law whose index is determined by the shock conditions, with $x = 3/(6-n)$,[7] whereas our IMF contains two contributions: a pure power law, of index $x = (n+1)/(2n-4)$, and a lognormal contribution resulting in an exponential decrease at the injection scale, as stated by equations (36) and (43). Interestingly, in the Padoan & Nordlund theory, x increases with n, whereas in our case, x *decreases* with n. This fundamental difference is due to the fact that in the Padoan & Nordlund theory, turbulence is always promoting star formation, since turbulent support is not included, whereas in our case, turbulence is also supporting the gas against gravitational collapse, leading globally to a negative effect on star formation, as shown in § 6.3. Testing these qualitatively different predictions on the n-dependence would bring precious information on the very role of turbulence in star formation.

Our theory also explains why hydrodynamical simulations of turbulence do recover the correct Salpeter power-law slope at high masses (Tilley & Pudritz 2004; Bate & Bonnell 2005). It is also in agreement with the finding that the CMF/IMF depends on the Mach number (Ballesteros-Paredes et al. 2006).

Finally, our approach provides a consistent explanation, within the same general framework, for the mass distribution of both self-gravitating structures and CO clumps. This fits well the recent results of Dib et al. (2008), where it is shown that clouds defined by a low-density threshold present a flat mass spectrum of index $\simeq -1.7$, whereas clouds having a higher degree of gravitational binding and defined by a higher density threshold have a stiffer mass spectrum.

7.3. *Restriction of the Present Work*

It is necessary to emphasize various limitations of our present theory. These issues require further detailed investigations. First of all, as known in the cosmological context, the window function used to perform the smoothing at scale R has some influence on the results (e.g., Nagashima 2001). The same is true for the probability $P(M, M')$ of finding a structure of mass M inside a structure of mass M', as demonstrated by Jedamzik (1995), although Jedamzik finds a relatively modest influence of $P(M, M')$ (although see Yano et al. 1996; Nagashima 2001). Second of all, the turbulent Jeans mass is treated using a mean scale dependence. Ideally, this could be improved by considering a velocity distribution correlated to the density. The same is true for the magnetic field distribution.

At last, another important aspect already mentioned in §4.5, ignored in this work as in most of the other theories of the IMF, is the time dependence issue in the star formation process. The present theory consists simply in counting the fluctuations of a given distribution, produced by an underlying density field. In principle, the density fluctuations should evolve with time and rejuvenate. In particular, one may wonder whether the small scales should not rejuvenate more rapidly than the larger one. We think that part of the answer comes from the assumption of ergodicity, which states that spatial averaging should give the same results as time

[7] We recall that n is here the three-dimensional value of the power spectrum index. It thus corresponds to $n = \beta + 2$ in the Padoan & Nordlund theory, where $x = 3/(4-\beta)$.

averaging. In particular, the ratio of small- to large-scale fluctuations should remain the same. This is, however, obviously not the case for the scales comparable to the size of the cloud itself. For those, a time-dependent theory seems unavoidable.

In a related way, our approach does not consider any accretion from external sources nor any further fragmentation during the collapse. Both could make the IMF different from the CMF, although the magnetic field seems to reduce the fragmentation significantly (Hennebelle & Teyssier 2008; Machida et al. 2008; Price & Bate 2008). On the other hand, the observed strong similarity between the CMF and the *system* IMF suggests that the latter is determined essentially by the CMF and that its shape should not be drastically modified by accretion, other than for the matter already included in the core reservoir. As for subfragmentation of the cores into individual objects, it has been shown that taking into account the mass-dependent multiplicity frequencies observed in the solar neighborhood seems to provide the correct link between the IMF of unresolved systems and the one of resolved individual objects (Chabrier 2003a, 2003b). We expect the same to be true for our theoretical CMF/IMF, although identifying the exact physical processes responsible for this subfragmentation remains an open issue.

8. CONCLUSION

In the present paper we have derived an analytical theory for the stellar IMF and for the mass function of the CO clumps, based on an extension of the statistical Press-Schechter formalism derived in cosmology. Our theory provides a *predictive* theoretical foundation to understand the origin of the stellar IMF and to infer its behavior in various environments. The theory predicts that the CMF/IMF involves two contributions, namely, a power-law tail and an exponential cutoff below about the mean thermal or turbulent Jeans mass, even in the absence of turbulence. Although thermal collapse produces too steep a slope compared with the Salpeter value, the latter is recovered exactly in the case of supersonic turbulence, for the appropriate observed or numerically determined power spectrum index. This corroborates the general gravoturbulent picture of star formation, as initiated by Larson (1981) and developed more recently by Padoan & Nordlund (2002), where large-scale protostellar clumps which contain several Jeans masses are dominated by supersonic turbulent motions and will fragment into prestellar cores that produce the final stellar spectrum. The smaller clumps will have subsonic internal velocities, in agreement with the observed Larson's relations in molecular clouds, i.e., will be supported by thermal motions, leading to a turnover of the CMF/IMF about the characteristic effective Jeans mass. Turbulence favors the formation of both low-mass and high-mass structures, but as a whole, it has a negative effect on star formation, decreasing the overall star formation efficiency. We also suggest that the opposite, comparable scale dependences of the Mach number and Jeans mass lead to a weak dependence of the location of the peak of the IMF on clump masses, providing an appealing explanation for the observed rather universal behavior of the IMF over a wide range of stellar cluster conditions.

The success of the present theory in reproducing the CMF/IMF inferred from the observations of prestellar cores strongly suggests that the IMF is determined by the conditions prevailing in the cloud, temperature, density, and scale dependence of the velocity dispersion (i.e., characteristic velocity power spectrum) and, thus, is already imprinted at early stages in the cloud. The universality of the IMF, at least under present-day Galactic conditions, very likely arises from the universality of the self-similar nature of turbulence and from comparable characteristic cloud conditions, determined by the same dominant cooling processes. Effects like accretion, ejection, collisions, and winds may affect to some extent the exact shape of the CMF/IMF, explaining possible statistical variations, but are unlikely to be dominant mechanisms.

We are grateful to Philippe André, Sami Dib, Bruce Elmegreen, Wolfram Schmidt, and Enrique Vázquez-Semadeni for insightful comments and for a critical reading of the manuscript, to Edouard Audit for stimulating discussions, to Paolo Padoan and Åake Nordlund for lively e-mail exchanges, and to the anonymous referee for helpful comments. P. H. thanks Alexei Kritsuk for many stimulating discussions on turbulence during his stay at the Kavli Institute for Theoretical Physics and for providing the power spectrum of log ρ calculated with his state-of-the-art hydrodynamical simulations. He is also very grateful to Chris McKee and Shu-ichiro Inutsuka for many discussions on related topics over the years. G. C. acknowledges the warm hospitality of the Max Planck Institute for Astrophysics and numerous discussions with various colleagues. This work was supported by the French "Agence Nationale pour la Recherche" (ANR) within the "Magnetic Protostars and Planets" (MAPP) project and by the "Constellation" European Network grant MRTN-CT-2006-035890.

APPENDIX A

MASS SPECTRUM OF VOIDS

Here, we show that the voids have the same mass spectrum as the structures. The voids are regions of gas where the density is smaller than the average density. The mass contained within structures of mass smaller than $M_R = \rho_c R^3$ is given by

$$M_{\rm tot}(R) = L_i^3 \int_{-\infty}^{\delta_c} \bar{\rho} \exp(\delta) \mathcal{P}_R(\delta) d\delta, \tag{A1}$$

while equation (10) remains applicable. Thus,

$$\mathcal{N}(M_R) = -\frac{2\bar{\rho}}{M_R} \frac{dR}{dM_R} \frac{1}{\sqrt{2\pi}\sigma^2} \frac{d\sigma}{dR} \int_{-\infty}^{\delta_c} A(\delta, R) d\delta. \tag{A2}$$

From equation (15), we see that

$$\int_{-\infty}^{\infty} A(\delta, R) d\delta = 0. \tag{A3}$$

This implies that

$$\int_{-\infty}^{\delta_c} A(\delta, R)d\delta = -\int_{\delta_c}^{\infty} A(\delta, R)d\delta. \tag{A4}$$

Therefore, the mass spectrum of voids is given by

$$\mathcal{N}(M) = \frac{\bar{\rho}}{M^2}\left(\frac{M}{M_0}\right)^{(n'-3)/3}\left(\frac{\bar{\rho}}{\rho_c}\right)^{(n'-3)/3}\frac{(n'-3)\sigma_0^2}{3\sqrt{2\pi}\sigma^3}\left(-\delta_c - \frac{\sigma^2}{2}\right)\exp\left[-\frac{(\delta_c - \sigma^2/2)^2}{2\sigma^2}\right]. \tag{A5}$$

APPENDIX B

THE $d\mathcal{P}_R/dR$ TERM

Here, we investigate the role played by the second term which appears in equation (33). From equations (12), (15), (29), (28), and equation (33), equation (43) should be

$$\mathcal{N}(\tilde{M}) = 2\mathcal{N}_0\frac{1}{\tilde{R}^3}\frac{1}{1+(2\eta+1)\mathcal{M}_*^2\tilde{R}^{2\eta}}\left[\frac{1+(1-\eta)\mathcal{M}_*^2\tilde{R}^{2\eta}}{\left(1+\mathcal{M}_*^2\tilde{R}^{2\eta}\right)^{3/2}} - \frac{\delta_R^c + \sigma^2/2}{\left(1+\mathcal{M}_*^2\tilde{R}^{2\eta}\right)^{1/2}}\frac{n'-3}{4}\frac{\sigma_0^2}{\sigma^2}\left(\frac{\tilde{R}}{\tilde{L}_i}\right)^{n'-3}\right]$$
$$\times \exp\left\{-\frac{\left[\ln\left(\tilde{M}/\tilde{R}^3\right)\right]^2}{2\sigma^2}\right\}\frac{\exp(-\sigma^2/8)}{\sqrt{2\pi}\sigma}, \tag{B1}$$

where $\tilde{L}_i = L_i/\lambda_{\mathrm{J}}^0$ and where, for simplicity, we have assumed that $n = n'$. We thus see that the second term becomes comparable to the first one only when $(\tilde{R}/\tilde{L}_i)^{n-3}\sigma_0^2/\sigma^2(\tilde{R}) \simeq 1$, which happens when $R \simeq L_i$, i.e., for structures whose size is comparable to the injection scale, expected to be the size of the whole system.

APPENDIX C

ON THE $P(M, M') = 1/2$ RESULT

Here, we justify that, as in Yano et al. (1996), for a window function sharply truncated in the k-space, one has $P(M, M') = 1/2$. Let us consider a subregion of the flow which, smoothed at scale R', has a density equal to ρ_c. This subregion is also following a Gaussian statistics in the variable $\delta = \log(\rho/\rho_c)$. Let $M' \simeq \rho_c(R')^3$. The probability that a region of size $R < R'$ has a density larger than ρ_c and thus contains a mass larger than M_R^c is given by

$$P\left(M_R^c, M'\right) = \int_0^{\infty}\frac{1}{\sqrt{2\pi}}\frac{1}{\sigma_{\mathrm{sub}}}\exp(\delta)\exp\left[-\frac{1}{2}\left(\frac{\delta + \sigma_{\mathrm{sub}}^2/2}{\sigma_{\mathrm{sub}}}\right)^2\right]d\delta,$$
$$= \int_{-\sigma_{\mathrm{sub}}/(2\sqrt{2})}^{\infty}\frac{1}{\sqrt{\pi}}\exp\left(-u^2\right)du, \tag{C1}$$

where $\sigma_{\mathrm{sub}} = \sigma^2(R') - \sigma^2(R)$. Since $R' \ll L_i$, one has $\sigma_{\mathrm{sub}} \ll \sigma_0$, thus $\sigma_{\mathrm{sub}} \simeq 0$. Indeed, this shows that $P(M_R^c, M') = 1/2$.

APPENDIX D

ON THE $P(R, M) = 1$ ASSUMPTION

Here, we give justifications of the $P(R, M) = 1$ assumption used in the paper. Let us consider a spherical cloud with a density profile $\rho \propto r^{-a}$. The cloud mass thus grows with r as $M(r) \propto r^{3-a}$.

The thermal Jeans mass, M_{J}, is proportional to $1/\sqrt{\rho}$, and thus, $M_{\mathrm{J}} \propto r^{a/2}$. This implies that

$$\frac{M_{\mathrm{J}}(r)}{M(r)} \propto r^{(3/2)a-3}. \tag{D1}$$

Therefore, if $a < 2$, the Jeans mass grows with r less rapidly than $M(r)$ and a Jeans unstable mass is thus embedded into a larger more gravitationally unstable cloud. This is precisely the assumption $P(R, M) = 1$.

In the case of turbulent support, $M_{\mathrm{J}}(r) \propto (C_{s,\mathrm{eff}})^3/\sqrt{\rho}$, and $M_{\mathrm{J}}(r) \propto r^{3\eta+a/2}$. Thus, the Jeans mass grows less rapidly than $M(r)$ if $3\eta + (3/2)a - 3 < 0$, leading to $a < 2 - 2\eta$. With $\eta \simeq 0.4$–0.5, this yields $a < 1$–1.2. Since it seems reasonable to assume that most cloud density profiles should not be much stiffer than $1/r^{(1-2)}$, we conclude that our assumption $P(R, M) = 1$ is realistic.

REFERENCES

Adams, F., & Fatuzzo, M. 1996, ApJ, 464, 256
Alves, J., Lombardi, M., & Lada, C. 2007, A&A, 462, L17
André, P., Basu, S., & Inutsuka, S-I. 2008, in Structure Formation in Astrophysics, ed. G. Chabrier (Cambridge: Cambridge Univ. Press), in press (arXiv: 0801.4210)
André, P., Belloche, A., Motte, F., & Peretto, N., 2007, A&A, 472, 519
Audit, E., Teyssier, R., & Alimi, J.-M. 1997, A&A, 325, 439
Ballesteros-Paredes, J., Gazol, A., Kim, J., Klessen, R., Jappsen, A.-K., & Tejero, E. 2006, ApJ, 637, 384
Basu, S., 2000, ApJ, 540, L103
Basu, S., & Jones, C. 2004, MNRAS, 347, L47
Bate, M., & Bonnell, I. 2005, MNRAS, 356, 1201
Bayly, B., Levermore, C., & Passot, T. 1992, Phys. Fluids, 4, 945
Bensch, F., Stutski, J., & Ossenkopf, V. 2001, A&A, 366, 636
Beresnyak, A., Lazarian, A., & Cho, J. 2005, ApJ, 624, L93
Blitz, L. 1993, in Protostars & Planets III, ed. E. H. Levy & J. I. Lunine (Tucson: Univ. Arizona Press), 125
Bonazzola, S., Heyvaerts, J., Falgarone, E., Pérault, M., & Puget, J. L. 1987, A&A, 172, 293
Bond, J., Cole, S., Efstathiou, G., & Kaiser, N. 1991, ApJ, 379, 440
Bower, R. 1991, MNRAS, 248, 332
Burgers, J. 1974, The Nonlinear Diffusion Equation (Dordrecht: Reidel)
Caselli, P., & Myers, P. 1995, ApJ, 446, 665
Chabrier, G. 2003a, PASP, 115, 763
———. 2003b, ApJ, 586, L133
———. 2005, in The Initial Mass Function 50 Years Later, ed. E. Corbelli & F. Palla (Dordrecht: Springer), 41
Chandrasekhar, S. 1951, Proc. R. Soc. London A, 210, 26
Crutcher, R. 1999, ApJ, 520, 706
Dib, S., Brandenburg, A., Kim, J., Gopinathan, M., & André, P. 2008, ApJ, 678, L105
Dib, S., Kim, D., & Shadmehri, M. 2007a, MNRAS, 381, L40
Dib, S., Kim, D., Vàzquez-Semadeni, E., Burkert, A., & Shadmehri, M. 2007b, ApJ, 661, 262
Efstathiou, G., Frenk, C., White, S., & Davies, M., 1988, MNRAS, 235, 715
Elmegreen, B. 1997, ApJ, 486, 944
———. 2007, ApJ, 668, 1064
Elmegreen, B., Klessen, R., & Wilson, C. 2008, ApJ, 681, 365
Glover, S., & Mac Low, M. 2007, ApJS, 169, 239
Heithausen, A., Bensch, F., Stutzki, J., Falgarone, E., & Panis, J.-F. 1998, A&A, 331, L65
Heitsch, F., Hartmann, L., Slyz, A., Devriendt, J., & Burkert, A. 2008, ApJ, 674, 316
Hennebelle, P., & Audit, E. 2007, A&A, 465, 431
Hennebelle, P., Mac Low, M.-M., & Vázquez-Semadeni, E.. 2008, in Structure Formation in Astrophysics, ed. G. Chabrier (Cambridge: Cambridge Univ. Press), in press (arXiv: 0711.2417)
Hennebelle, P., & Teyssier, R. 2008, A&A, 477, 25
Inutsuka, S.-I. 2001, ApJ, 559, L149
Jedamzik, K. 1995, ApJ, 448, 1
Johnstone, D., Wilson, C., Moriarty-Schieven, G., Joncas, G., Smith, G., Gregersen, E., & Fich, M. 2000, ApJ, 545, 327
Kim, J., & Ryu, D. 2005, ApJ, 630, L45
Kramer, C., Stutzki, J., Rohrig, R., & Corneliussen, U. 1998, A&A, 329, 249
Kritsuk, A., Norman, M., Padoan, P., & Wagner, R. 2007, ApJ, 665, 416
Krumholz, M., & McKee, C. 2005, ApJ, 630, 250
Kroupa, P. 2002, Science, 295, 82
Lacey, C., & Cole, S. 1993, MNRAS, 262, 627
Larson, R. 1973, MNRAS, 161, 133
———. 1981, MNRAS, 194, 809
Lequeux, J. 2005, The Interstellar Medium (Berlin: Springer)
Li, P. S., Norman, M. L., Mac Low, M., & Heitsch, F. 2004, ApJ, 605, 800
Luhman, K. 2004, ApJ, 630, 1216
———. 2007, ApJS, 173, 104
Mac Low, M.-M., & Klessen, R. 2004, Rev. Mod. Phys., 76, 125
Machida, M., Tomisaka, K., Matsumoto, T., & Inutsuka, S.-I. 2008, ApJ, 677, 327
Matzner, C. D., & McKee, C. 2000, ApJ, 545, 364
McKee, C. 1999, The Origin of Stars and Planetary Systems, ed. C. J. Lada & D. Kylafis (Dordrecht: Kluwer), 29
Miller, G., & Scalo, J. 1979, ApJS, 41, 513
Moraux, E., Bourier, J., & Clarke, C. 2005, Astron. Nachr., 326, 985
Motte, F., André, P., & Neri, R. 1998, A&A, 336, 150
Motte, F., Bontemps, S., Schilke, P., Schneider, N., Menten, K. M., & Broguière, D. 2007, A&A, 476, 1243
Myers, P., & Goodman, A. 1988, ApJ, 326, L27
Nagashima, M. 2001, ApJ, 562, 7
Ostriker, E., Stone, J., & Gammie, C. 2001, ApJ, 546, 980
Padmanabhan, T. 1993, Structure Formation in the Universe (Cambridge: Cambridge Univ. Press)
Padoan, P., & Nordlund, Å. 1999, ApJ, 526, 279
———. 2002, ApJ, 576, 870
Padoan, P., Nordlund, Å., & Jones, B. 1997, MNRAS, 288, 145
Padoan, P., Nordlund, Å., Kritsuk, A., Normam, M., & Li, P.-S. 2007, ApJ, 661, 972
Passot, T., & Vázquez-Semadeni, E. 1998, Phys. Rev. E, 58, 4501
Passot, T., Vázquez-Semadeni, E., & Pouquet, A. 1995, ApJ, 455, 536
Peretto, N., Hennebelle, P., & André, P. 2007, A&A, 464, 983
Press, W., & Schechter, P. 1974, ApJ, 187, 425 (PS74)
Price, D., & Bate, M. 2008, MNRAS, 385, 1820
Salpeter, E. 1955, ApJ, 121, 161
Silk, J. 1995, ApJ, 438, L41
Spitzer, L., 1978, Physical Processes in the Interstellar Medium (New York: Wiley)
Stutzki, J., Bensch, F., Heithausen, A., Ossenkopf, V., & Zielinsky, M. 1998, A&A, 336, 697
Testi, L., & Sargent, A. 1998, ApJ, 508, L91
Tilley, D., & Pudritz, R. 2004, MNRAS, 353, 769
Vázquez-Semadeni, E. 1994, ApJ, 423, 681
Vázquez-Semadeni, E., & Gazol, A. 1995, A&A, 303, 204
Vázquez-Semadeni, E., González, R., Ballesteros-Paredes, J., Adriana, G., & Jongsoo, K. 2008, MNRAS, submitted
Vázquez-Semadeni, E, Kim, J., & Ballesteros-Paredes, J. 2005, ApJ, 630, L49
Yano, T., Nagashima, M., & Gouda, N. 1996, ApJ, 466, 1
Zinnecker, H. 1984, MNRAS, 210, 43